

Synthesis, characterization, and solid-state polymerization of cross-conjugated octatetraynes

Yuming Zhao, Thanh Luu, Guy M. Bernard, Tyler Taerum, Robert McDonald, Roderick E. Wasylishen, and Rik R. Tykwinski

Abstract: Two series of cross-conjugated 1,3,5,7-octatetraynes (**1a–1l** and **6a–6d**) have been synthesized. UV–vis spectroscopic analysis shows that pendent groups connected to the cross-conjugated skeleton have little effect on the λ_{\max} energies, irrespective of whether the groups are electron withdrawing or donating. A number of the isolated products readily give crystals suitable for X-ray crystallography, and the solid-state structural properties of five derivatives (**1k**, **1l**, **6a**, **6c**, and **6d**) have been examined by X-ray crystallographic analysis. Parallel packing of the polyynes in the solid state indicates that four of the five samples are potentially suitable for topochemical polymerization, based on solid-state packing parameters θ , R , and d . Attempts to effect a solid-state reaction have been explored through UV–vis and γ -ray irradiation as well as thermal heating. The course of these reactions was monitored by differential scanning calorimetry (DSC) analysis, as well as UV–vis and solid-state ^{13}C NMR spectroscopy (for **1d**, **1j**, **1k**, and **6d**), which offered evidence of polymer formation from these reactions. Structural determination of the product(s), however, remains elusive.

Key words: polytriacylenes, polyynes, solid-state NMR spectroscopy, tetraynes, topochemical polymerization.

Résumé : On a réalisé la synthèse de deux séries de 1,3,5,7-octatétraynes à conjugaisons croisées (**1a–1l** et **6a–6d**). L'analyse de leurs spectres UV–visible montre que les groupes pendants attachés au squelette à conjugaison croisée n'ont que peu d'effet sur les énergies des λ_{\max} , que les groupes attachés soient électroaffinitaires ou électrorépulseurs. Un certain nombre de produits isolés fournissent des cristaux susceptibles d'être soumis à une diffraction par des rayons-X; on a ainsi pu déterminer les propriétés structurales de cinq dérivés (**1k**, **1l**, **6a**, **6c** et **6d**) par une analyse des données cristallographiques par cette méthode. L'entassement parallèle des polyynes à l'état solide indique que quatre des cinq échantillons pourraient éventuellement être susceptibles de donner lieu à une polymérisation topochimique si on se base sur leurs paramètres d'empilement θ , R et d . On a exploré la possibilité de réaliser des réactions à l'état solide par des irradiations UV–visible et par des rayons γ ainsi que par un chauffage thermique. On a suivi le cours de ces réactions par le biais d'une analyse par calorimétrie à balayage différentiel (CBD) ainsi que par les spectroscopies UV–visible et RMN du ^{13}C à l'état solide (pour les composés **1d**, **1j**, **1k** et **6d**) qui fournissent des données suggérant qu'il y a formation de polymères au cours de ces réactions. La détermination des structures de ces produits demeure toutefois incertaine.

Mots-clés : polytriacylènes, polyynes, spectroscopie RMN à l'état solide, tétraynes, polymérisation topochimique.

[Traduit par la Rédaction]

Introduction

During the past couple of decades, solid-state polymerization of polyynes has been the subject of considerable exploration in the quest for conjugated organic materials with qualities suitable for applications in nanoscience, nonlinear optics, organic electronics, supramolecular chemistry, and sensing.^{1–8} Solid-state polymerization of polyynes is an attractive route to such materials because it can provide large and nearly defect-free polymer crystals, as well as materials

with unique solution-state properties.^{9–11} The topochemical polymerization of a “diacetylene” (diyne) monomer into a polydiacetylene polymer was first reported by Wegner¹² in 1969. In the intervening years, the breadth of this general process has been studied and expanded. These investigations have documented quite clearly that the solid-state packing of the polyyne precursor in the crystalline state is crucial to formation of the desired polymer.^{13–16} In polyyne crystals, molecules must move cooperatively during the reaction process to arrive at the ordered structure of the polymeric product

Received 17 February 2012. Accepted 28 June 2012. Published at www.nrcresearchpress.com/cjc on 30 November 2012.

Y. Zhao. Department of Chemistry Memorial University of Newfoundland, St. John's, NL A1B 3X7, Canada.

T. Luu, G.M. Bernard, T. Taerum, and R.E. Wasylishen. Department of Chemistry, University of Alberta, Edmonton, AB T6G 2G2, Canada.

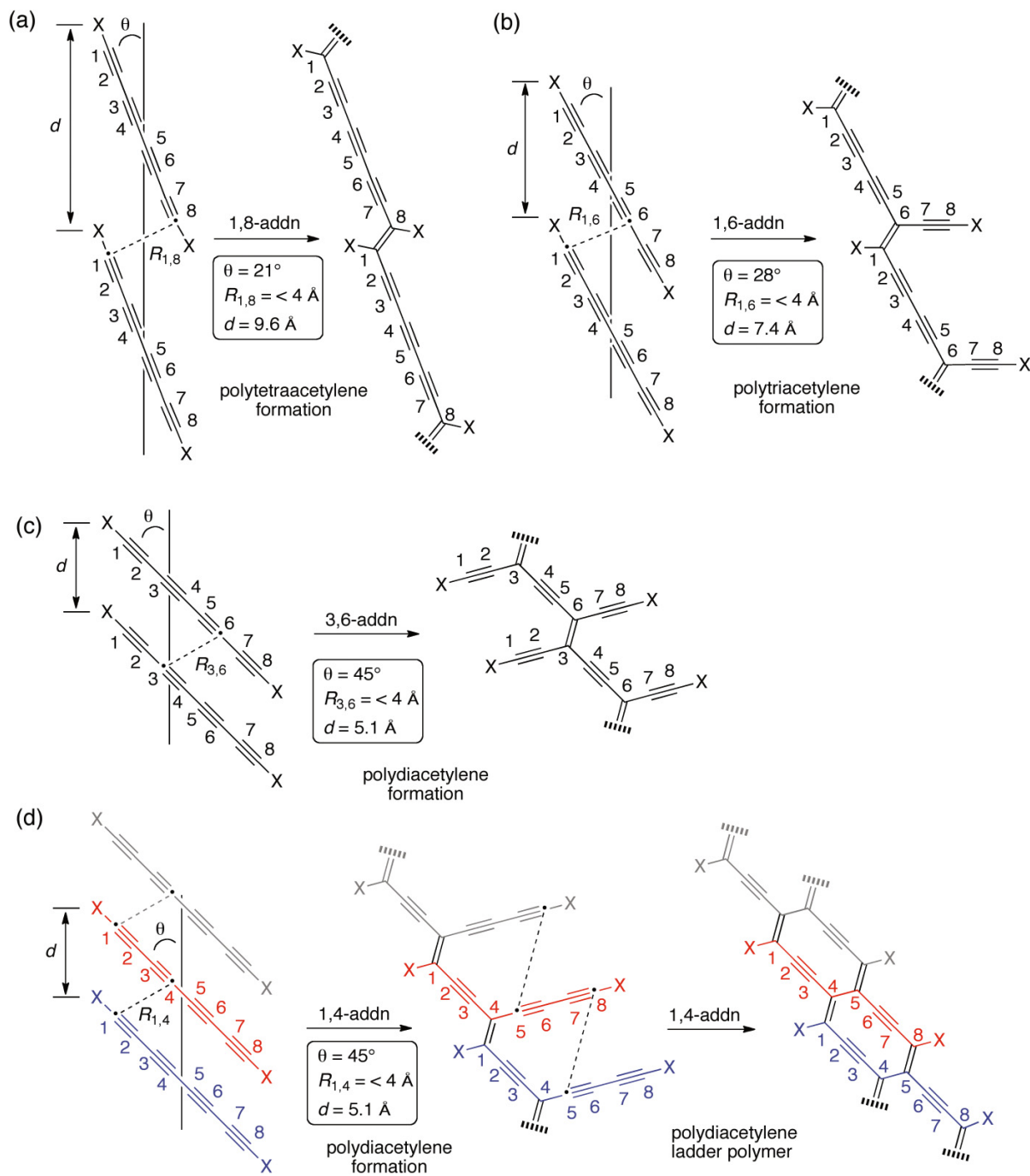
R. McDonald. X-ray Crystallography Laboratory, Department of Chemistry, University of Alberta, Edmonton, AB T6G 2G2, Canada.

R.R. Tykwinski. Department of Chemistry and Pharmacy & Interdisciplinary Center of Molecular Materials (ICMM), University of Erlangen-Nuremberg, Henkestrasse 42, 91054 Erlangen, Germany.

Corresponding author: Rik R. Tykwinski (e-mail: rik.tykwinski@chemie.uni-erlangen.de).

Dedicated to Professor Derrick Clive in recognition of a lifetime of contributions to organic synthesis.

Fig. 1. Schematic crystal packing for several modes of octatetrayne polymerization, and optimal parameters θ , R , and d for each addition pattern. (a) Polytetraacetylene formation via 1,8-addition. (b) Polytriacetylene formation via 1,6-addition. (c) Polydiacetylene formation via 3,6-addition. (d) Ladder polymer formation via two sequential 1,4-additions.

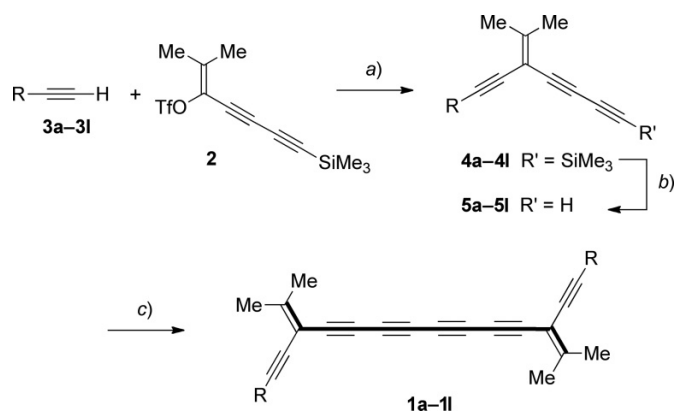


(i.e., a phase transition). When the solid-state arrangement of the polyynes offers a reaction pathway with minimal translational energy, a topochemical reaction is possible when initiated by, for example, heat, UV light, pressure, or γ -ray radiation. Such reactions are common for diynes and selectively form the polydiacetylene product. For longer polyynes precursors, however, multiple reaction possibilities exist, as schematically shown in Fig. 1 for tetraynes. Thus, while polyynes precursors offer a tantalizing opportunity to form

highly conjugated polymer products,^{15,17,18} the various modes of reactivity present a number of challenges, including the realization of the single crystals with optimal packing parameters, dictating one particular reaction pathway to the exclusion of another, and characterization of the often insoluble reaction product(s).

Efforts to effect polymerization of polyynes beyond the length of a diyne have been relatively rare, although several examples are described for the polymerization of triynes,¹⁹

Scheme 1. Synthesis of tetraynes **1a–1l**. Reagents and conditions: (a) PdCl₂(PPh₃)₂, CuI, *i*-Pr₂NH, THF, rt; (b) K₂CO₃, MeOH, THF; (c) CuCl, TMEDA, acetone or acetone/CH₂Cl₂ (1:1), O₂ (air), rt. The longest linearly conjugated segment is highlighted in bold. THF, tetrahydrofuran; TMEDA, tetramethylethylenediamine.



pentaynes,²⁰ and hexaynes.²¹ There has been slightly more work done in the area of tetraynes,²² likely because of the fact that tetraynes are both easy to synthesize and relatively stable under ambient conditions.²³ In considering the topochemical polymerization of tetraynes, several pathways must be considered, as outlined in Fig. 1. In each case, packing parameters based on the orientation of neighbouring molecules stacked parallel in the solid state govern reactivity patterns that might be energetically accessible. The packing parameters are defined as (i) the stacking or translational distance of the monomers in the parallel stack (d), (ii) the angle formed between the polyyne and the stacking axis (the “tilt angle”; θ), and (iii) the distance between the reacting carbon atoms in neighbouring molecules of the stack (R).^{13,15} For example, 1,8-addition for a tetrayne gives a polytetraacetylene product (Fig. 1a), whereas 1,6-addition forms a polytriacetylene²⁴ product (Fig. 1b). A variety of reaction pathways are possible that would result in polydiacetylene formation via a formal 1,4-addition pattern, such as those in Figs. 1c and 1d, which afford interesting cross-conjugated polymers.²⁵ It is noteworthy that topochemical polymerization can also lead to polydiacetylene “ladder polymers” through two sequential 1,4-polymerization events (Fig. 1d).^{17b} As part of an ongoing interest in the structural and electronic properties of cross-conjugated enyne systems,^{25a,26} we serendipitously discovered that a large number of cross-conjugated tetrayne products crystallize with the polyynes stacked in parallel, with packing parameters potentially suitable for topochemical polymerization. Thus, we report herein on the synthesis and study of two series of tetraynes, the spectroscopic characterization of these compounds, our efforts to polymerize these polyynes, and difficulties encountered in the characterization of the product(s) of these solid-state reactions.

Synthesis

Notably, the synthesis of the cross-conjugated tetrayne series **1a–1l** is achieved in three efficient steps, as described in Scheme 1 and summarized in Table 1.²⁷ First, Pd-catalyzed Sonogashira cross coupling²⁸ of the known vinyl triflate **2**²⁹ with various terminal acetylenes (**3a–3l**) gave enynes **4a–4l**.

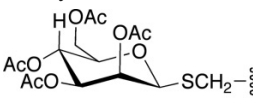
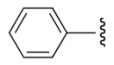
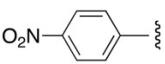
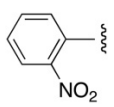
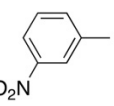
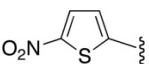
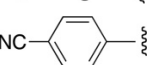
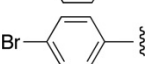
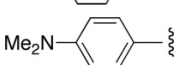
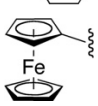
These reactions generally proceeded smoothly at room temperature (rt) and were complete within 2 h. Isolated yields of triynes **4a–4l** were good to excellent, and, with the exception of **4a** (an oil), triynes **4** are isolated as stable solids. Protodesilylation of **4a–4l** then provided the terminal alkynes **5a–5l**, which were carried on directly, following workup, to the oxidative homocoupling step using Cu-mediated Hay conditions.³⁰ The homocoupling reactions were typically complete in ~0.5 h at rt using either acetone or a mixture of acetone/CH₂Cl₂ (1:1) as solvent. Isolated yields for **1a–1l** ranged from excellent to poor, depending primarily on the stability of the resulting product. Nitroaryl functionalized tetraynes **1e–1g** had particularly poor stability, even at low temperature and in solution. This resulted in drastically reduced isolated yields for **1e** and **1f**, whereas **1g** was insufficiently stable for isolation. While *n*-butyl- and cyano-substituted tetraynes **1a** and **1h**, respectively, were also relatively unstable at room temperature, yields were nevertheless reasonable and the products could be handled without significant decomposition if kept in solution.

Next, our investigations of α,ω -polyynes³¹ led to the formation of the dibromoolefinic analog of tetrayne **1c**, namely **6a** (Scheme 2). Compound **6a** was isolated as a crystalline solid with interesting solid-state packing based on X-ray analysis (vide infra). This suggested a second class of octatetraynes that might be explored for their solid-state behaviour. Tetraynes **6a–6d** were easily synthesized starting from commercially available acid chlorides **7a–7d** as shown in Scheme 2 and summarized in Table 2. In the first step, a Friedel–Crafts acylation reaction of **7a–7d** with 1,4-bis-trimethylsilyl-1,3-butadiyne (**8**) in the presence of AlCl₃ afforded the intermediate ketones **9a–9d**, after quenching of the reaction and aqueous workup.³² The crude ketones were then converted directly to dibromoolefins **10a–10d** via the Ramirez olefination reaction.³³ Isolated yields were good to excellent over the two steps, and **10a–10d** were obtained as stable crystalline solids. With diyne precursors **10a–10d** in hand, desilylation using K₂CO₃/MeOH gave the terminal alkynes, which were carried on directly to Hay³⁰ homocoupling in CH₂Cl₂. The desired products (**6a–6d**) were isolated pure in good to moderate yields by either column chromatography or recrystallization from hexanes.

¹³C-labelling of compound 6d

It is well-established that solid-state ¹³C NMR spectroscopy can provide invaluable structural information concerning the products of topochemical polymerization reactions.³⁴ With this in mind, the synthesis of tetrayne **6d** enriched with ¹³C atoms was undertaken (Scheme 3). The synthesis began with the known dibromoolefin **11**,³⁵ which incorporated ~34% ¹³C at position C(1) (indicated with an *). The reaction of the dibromoolefin **11** with excess lithium diisopropylamide (LDA) at low temperature effected elimination, and the resulting lithiated diyne product was trapped via the reaction with Me₃SiCl to give differentially silylated diyne **12**.³⁶ Following a similar reaction sequence as outlined in Scheme 2, diyne **12** was then converted into ketone **13** via a Friedel–Crafts acylation with **7d**, and the ketone was carried on directly to a standard dibromoolefination reaction affording dibromoolefin **14** in a reasonable yield (35%) over the two steps. The presence of the triisopropylsilyl group in **14** necessitated the use of

Table 1. Synthetic details and selective physical properties of enetriyne precursors **4a–4l** and tetraynes **1a–1l**.

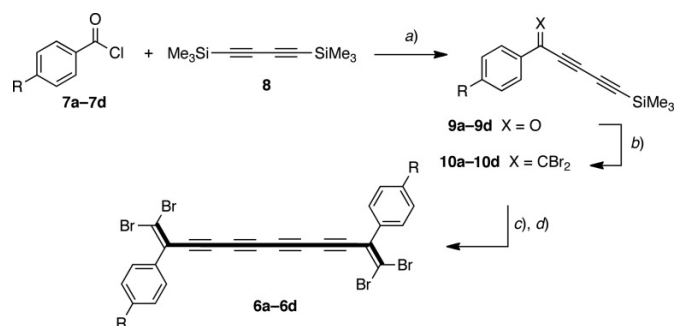
Entry	R	4		1		
		Yield (%)	Description (mp, °C) ^a	Yield (%)	Description (mp, °C) ^a	DSC, dp (<i>T</i> _{onset} / <i>T</i> _{max} ; °C)
a	<i>n</i> -Butyl	98	Unstable oil	94	Unstable oil	—
b		65	Colourless solid (54–57)	91	Brown solid (57–62)	—
c		96	Colourless solid (71–72)	66	Yellow, waxy solid	—
d		90	Yellow solid (94–95)	95	Yellow solid	172/193
e		87	Yellow solid (93–94)	27	Unstable, yellow semisolid	—
f		91	Yellow solid (77–78)	39	Unstable, yellow semisolid	—
g		36	Yellow solid (68–69)	0	—	—
h		80	Yellow solid (60–62)	74	Unstable, yellow solid	—
i		79	Colourless, waxy solid	85	Yellow solid	123/131
j		83	Yellow solid (82–83)	76	Yellow solid	157/165
k		56	Yellow solid (84–85)	75	Orange solid	160/187
l^b	<i>i</i> -Pr ₃ Si	93	Colourless solid (30–31)	96	Yellow solid (103–104)	145

Note: mp: melting point, DSC: differential scanning calorimetry, dp: decomposition, *T*: temperature.

^aMeasured in an open capillary tube.

^bSynthesized as reported in ref. 27.

Scheme 2. Synthesis of tetraynes **6a–6d**. Reagents and conditions: (a) AlCl₃, CH₂Cl₂, –20 °C; (b) CBr₄, PPh₃, CH₂Cl₂; (c) K₂CO₃, MeOH/THF; (d) CuCl, TMEDA, CH₂Cl₂, O₂ (air), rt. The longest linearly conjugated segment is highlighted in bold. THF, tetrahydrofuran; TMEDA, tetramethylethylenediamine.



tetrabutylammonium fluoride (TBAF) to effect desilylation, and the thus formed terminal diyne was then subjected to oxidative homocoupling under Hay conditions. As a result of

the partial labelling, three isotopomers were formed from the homocoupling reaction, including compound **6d** (no labelled carbon), **6d*** (one labelled carbon), and **6d**** (two labelled carbons). As expected, however, the ¹³C NMR spectrum of this mixture is identical to that of the unlabelled compound **6d**, except for the enhanced signal of the C(1) carbon of the octayne chain and the associated ¹³C–¹³C coupling (vide infra).

Solution-state ¹³C NMR spectroscopic characterization

Solution-state ¹³C NMR spectroscopy of compounds **1a–1l** shows that the α carbons of the isopropylidene backbone (Me₂C=C<) are easily identified because they are quite deshielded, resonating in the range of 160–165 ppm.³⁷ Electron-withdrawing aryl groups result in a downfield shift of this signal, such that the resonances of **1d** (4-NO₂-C₆H₄-), **1e** (2-NO₂-C₆H₄-), **1f** (3-NO₂-C₆H₄-), and **1h** (4-NC-C₆H₄-) are found at 163.9, 165.0, 163.4, and 163.6 ppm, respectively. Conversely, electron-donating groups result in a slight upfield shift of this carbon resonance, as with derivatives **1j** (4-NMe₂-

Table 2. Synthetic details and selective physical properties of diyne monomers **10a–10d** and tetraynes **6a–6d**.

Entry	R	10		6		DSC: mp/dp (°C); $T_{\text{onset}}/T_{\text{max}}$ (°C)
		Yield (%)	Description (mp, °C) ^a	Yield (%)	Description (dp, °C) ^a	
a	H	77	Colourless solid (85–87)	75	Yellow solid (185)	—; 191/192 (dp)
b	OMe	90	Off-white solid (72–74)	46	Yellow-green solid (168–170)	176 (mp); 176/179 (dp)
c	<i>t</i> -Bu	65	Yellow solid (96–98)	80	Yellow solid (168–179) ^b	190; ^c 230/233 (dp)
d	NO ₂	51	Off-white solid (80–83)	51	Yellow solid (~190)	—; 189/191 (dp)

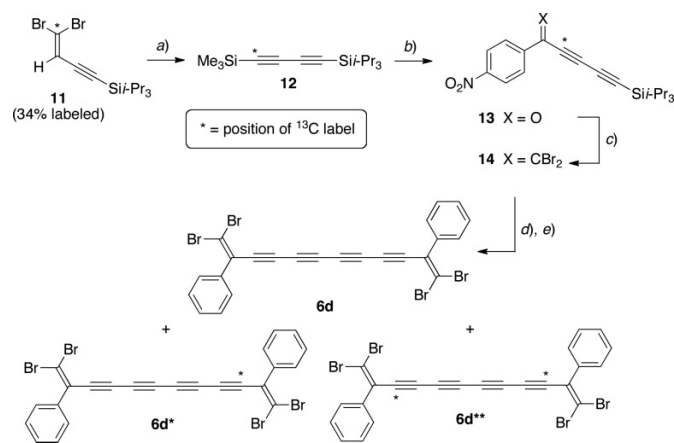
Note: mp: melting point, dp: decomposition, DSC: differential scanning calorimetry, T : temperature.

^aMeasured in an open capillary tube.

^bApparent melting point.

^cWeak exotherm.

Scheme 3. Synthesis of isotopomers **6d/6d*/6d****. Reagents and conditions: (a) LDA, THF, -78 °C, then Me₃SiCl, 67%; (b) **7d**, AlCl₃, CH₂Cl₂, -20 °C; (c) CBr₄, PPh₃, CH₂Cl₂, 0 °C, 35% (from **12**); (d) TBAF, THF, rt; (e) CuCl, TMEDA, CH₂Cl₂, O₂, rt, 42% (from **14**). LDA, lithium diisopropylamide; THF, tetrahydrofuran; TBAF, tetra-*n*-butylammonium fluoride; TMEDA, tetramethylethylenediamine.



C₆H₄–) and **1k** (ferrocenyl) at 159.5 and 159.9 ppm, respectively. The analogous carbons for tetraynes **6a–6d**, terminated with a dibromovinyl group (Br₂C=C<), are found at much lower chemical shift values, a result of the heavy atom effect, typically in the range of ~100 ppm based on published studies using ¹³C labelling.³⁸ This places the resonance in the region of the alkyne carbon signals and complicates unambiguous assignment for **6a–6d**. Empirically, however, signals observed for **6a–6d** (and **10a–10d**) in the range of 102–108 ppm are consistent with this assignment. Conversely, the β-alkylidene carbons (Me₂C=C<) for isopropylidene compounds such **1a–1l** are typically found in the range of 99–100 ppm,³⁷ and thus they are also difficult to conclusively discern from the alkyne carbon resonances. For compounds **6d** and **14**, the β-alkylidene carbon (Br₂C=C<) can be identified at 127.6 and 128.3 ppm, respectively, as a result of the large one-bond coupling ($^1J(^{13}\text{C}, ^{13}\text{C}) = 98$ Hz) in each case to the ¹³C-labelled carbon at C(1). This compares to one-bond $^1J(^{13}\text{C}, ^{13}\text{C})$ values of 34.6, 67.6, and 171.5 Hz for ethane, ethylene, and acetylene, respectively.³⁹

Generally, the resonances of carbons C(3) and C(4) of an octatetrayne moiety (–C(1)≡C(2)–C(3)≡C(4)–C≡C–C≡C–) are found upfield relative to those of C(1) and C(2).^{35,40,41} In

the case of **1a–1l**, this places C(3) and C(4) at either ~64 or 68 ppm, regardless of the substitution pattern. The adjacent carbons C(1) and C(2), on the other hand, resonate in the range of 74–77 ppm. A similar pattern is found for **6a–6d**, where labelling of **6d*/6d**** provides an opportunity to identify each specific carbon within this tetrayne series. The labelled carbon C(1) for **6d*/6d**** is observed at 75.6 ppm, and the large coupling with C(2) at δ 82.7 ($^1J(^{13}\text{C}, ^{13}\text{C}) = 187$ Hz) sets this carbon resonance. Coupling between C(1) and C(3) at 71.4 ppm is also clearly observed with $^2J(^{13}\text{C}, ^{13}\text{C}) = 32$ Hz, and C(4) is thus identified as the remaining resonance at 64.9 ppm.

Solution-state UV-vis spectroscopic characterization

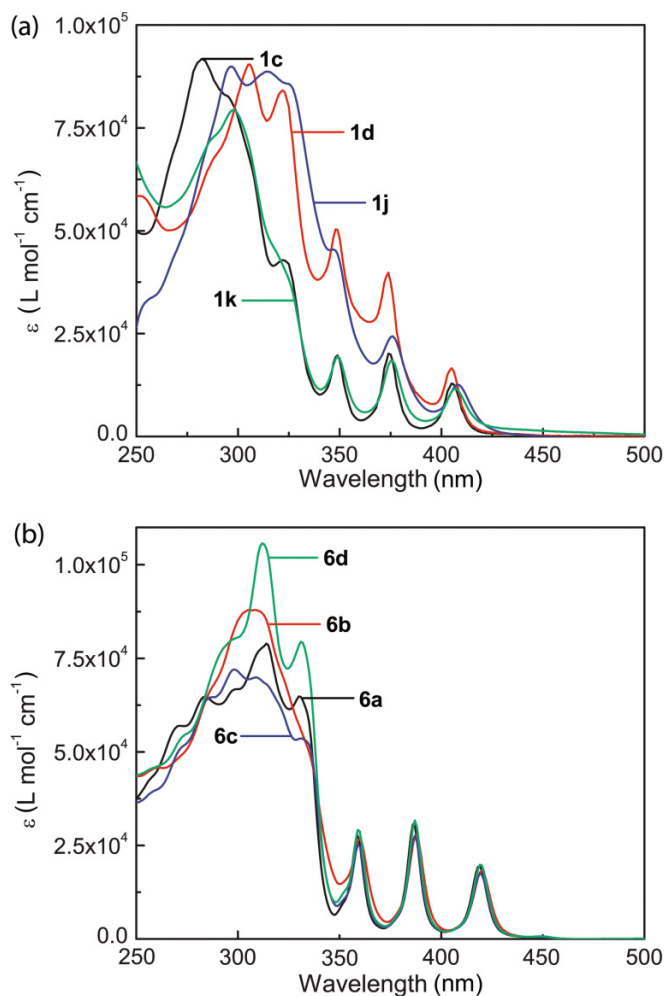
Highest occupied and lowest unoccupied molecular orbital (HOMO–LUMO) transitions for **1a–1l** and **6a–6d** should result from the longest linearly conjugated segment of these molecules (the ene–tetrayne–ene group highlighted in bold, Schemes 1 and 2).²⁷ In **1a–1l**, there is a progression of three absorptions at approximately 350, 375, and 405 nm (Fig. 2a). The various pendent functional groups have a negligible effect on the energy of these transitions as a result of the cross-conjugated framework.^{25–27,42} The most distinguishing effect based on structure is observed for derivatives with strong electron withdrawing and donating substituents, **1d** and **1j**, respectively, where an enhancement in molar absorptivity is observed in comparison with other derivatives. For the organometallic member of the series (**1k**), a weak, broad peak at 450 nm is attributed to the absorption characteristic of the ferrocenyl groups.

All members of the second series of tetraynes **6a–6d** also display three peaks in the low-energy region of the spectra at ~359, 387, and 419 nm (Fig. 2b). In addition, all four compounds have similar molar absorptivity values (ϵ). Thus, for **6a–6d**, as observed for **1a–1l**, varying the pendent substituents does not appreciably influence the wavelength of maximum absorption (λ_{max}) values.

Solid-state properties and attempted topochemical polymerization

Looking at the kinetic and thermal stability of cross-conjugated tetraynes **1a–1l** and **6a–6d**, derivatives with 4-nitrophenyl (**1d**), 4-*N,N*-dimethylaminophenyl (**1j**), ferrocenyl (**1k**), and triisopropylsilyl (**1l**) substituents show sufficient stability for detailed study, as do all four compounds **6a–6d**. As described in the following sections, our studies to date

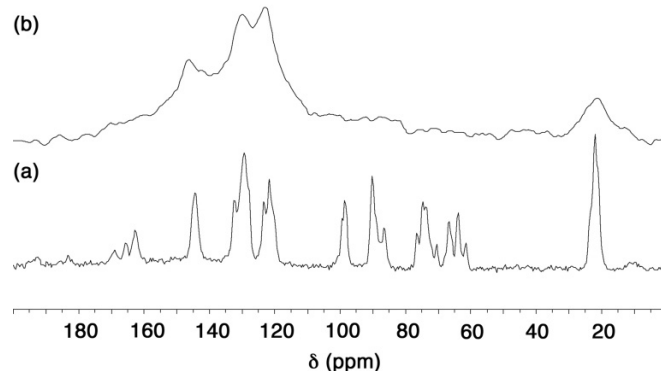
Fig. 2. Electronic absorption spectra (ϵ , L mol⁻¹ cm⁻¹) for (a) **1c**, **1d**, **1j**, and **1k** in CHCl₃ and (b) **6a–6d** in THF.



include differential scanning calorimetry (DSC) analysis for all eight of these compounds, X-ray crystallographic analysis of **1k**, **1l**, **6a**, **6c**, and **6d**, and solid-state ¹³C NMR spectroscopic analysis of **1d**, **1j**, **1k**, and **6d** during attempts to effect topochemical polymerization.

Last but not least, it is useful to point out several common threads from this study, as a prelude to the specific discussions that follow. Many reports for the solid-state reaction of polyynes have underscored the fact that the most important criteria for effective topochemical polymerization are the solid-state packing parameters θ , R , and d as summarized in Fig. 1. Supplemented with DSC analysis, this information offers, a priori, a guide for the selection of crystalline candidates for further study. It will become clear in the following sections, however, that a combination of suitable packing parameters and “sharp” DSC traces are only a part of the story for polymerization of tetrynes. As the solid-state ¹³C NMR spectroscopic studies eventually demonstrate, each “promising prospect” for thermal polymerization to a defined product results in only ambiguous evidence of the nature of the product, regardless of how “optimal” the packing parameters.

Fig. 3. Solid-state ¹³C NMR spectra for **1d** recorded (a) before heating and (b) after heating at 120 °C for 2 h and then 160 °C for 1 h.



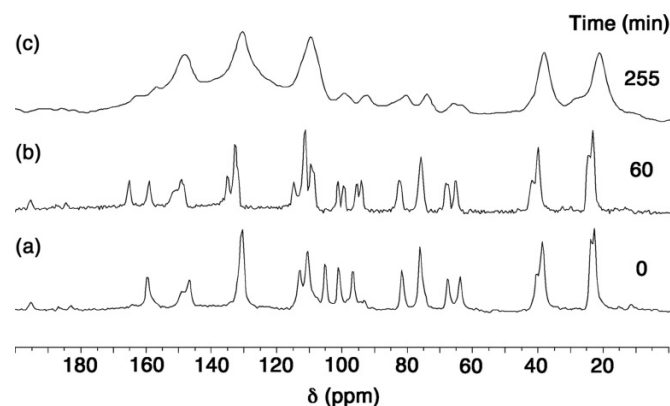
Tetryne **1d**

The DSC profile of **1d** shows a relatively broad and featureless Gaussian-shaped peak at 193 °C (see the Supplementary data), which suggests that the polymerization probably occurs in a random, nonregioselective manner. This premise has been examined by solid-state ¹³C NMR spectroscopy. The spectrum of pristine **1d** (Fig. 3a) shows moderate resolution, and major signals for the sp and sp² carbons in the region of 64–100 ppm are reasonably consistent with solution-state ¹³C NMR data. In addition to the expected resonances, however, several unidentified peaks are observed, likely the result of nonequivalent carbon atoms in the solid state (from a structure where C₂ symmetry has been lost). The same is true for the resonance of the external vinylidene carbon (Me₂C=C), which is observed at 164 ppm in addition to two additional signals at a similar chemical shift. After heating the sample of **1d** at 120 °C for 2 h, the resulting ¹³C NMR spectrum is identical to that of the original, indicating that polymerization had not occurred at this temperature. Subsequent heating at 160 °C for 1 h, on the other hand, gives a black solid. The spectrum of this product shows that the characteristic resonances for interior tetryne carbons at 64–67 ppm are completely gone after heating (Fig. 3b). While in agreement with a polymerized product, the loss of acetylenic signals coincides with the appearance of several broadened resonances in the region of 100–160 ppm, presumably the result of sp² carbons of olefinic and aryl moieties. In addition, the resonances of the methyl groups are also broadened significantly to a range of 15–30 ppm. The transition to broad featureless resonances, along with the absence of signals from sp carbon atoms, suggests that a random and nonregioselective polymerization occurs for this sample upon heating.

Tetryne **1j**

The DSC trace of **1j** shows a sharp exotherm at 165 °C (see the Supplementary data), suggesting that a solid-state reaction may be more regioselective than that observed for **1d**. In the absence of crystallographic data, the reaction has been explored by solid-state ¹³C NMR spectroscopy. The spectrum of **1j** at room temperature (Fig. 4a) shows reasonable resolution when compared to the solution-state ¹³C NMR spectrum. All eight unique sp and sp² carbons of the cross-conjugated enyne skeleton are clearly observed at 65, 68, 77, 82, 98, 102, 106,

Fig. 4. Solid-state ^{13}C NMR spectra for **1j** recorded (a) before heating (time = 0), (b) after heating at 100 °C for 60 min, and (c) after heating at 100 °C for 255 min.



and 160 ppm, while the two methyl carbons of the isopropylidene moiety are also distinct at 23 and 25 ppm. Finally, the *N,N*-dimethylanilino carbons are observed at 40 ppm. After heating at 100 °C for 1 h, the crystalline sample turns dark brown, and the ^{13}C NMR spectrum shows several distinct differences with fair resolution (Fig. 4b). The most significant changes upon heating are (i) the emergence of two nonequivalent vinylidene peaks at 159 and 165 ppm, (ii) splitting of the signal at 130 ppm, and (iii) several additional resonances in the range of 90–110 ppm. The characteristic resonances of the carbons of the polyynene fragment have approximately the same chemical shift values (in the region of 60–85 ppm), but they are broadened. Additional heating at 100 °C for ~3 h yields a black solid, the spectrum of which shows severely broadened signals, centred at 20, 40, 110, 130, and 150 ppm (Fig. 4c), although many of the major features observed in the initial spectrum after 60 min (Fig. 4b) are still distinguishable. In combination, these spectra suggest that polymerization may proceed in a regioselective manner, since distinct chemical shifts are still observed for the product (i.e., Fig. 4c). Several points deserve further discussion. If the reaction occurs via 1,6-addition, C_2 symmetry of the starting tetrayne would be destroyed while generating a polytriacetylene (PTA) product. The upfield signals at 60–70 ppm are not, however, consistent with the presence of a diyne group of a PTA. Alternatively, reaction via 1,8-addition would afford a polytetraacetylene product (Fig. 1a), and resonances in the ranges of 60–70 ppm could be consistent with the formation of an unsymmetrical triyne moiety.⁴³ Unfortunately, without crystallographic data of the starting material or product, more definitive conclusions are difficult to draw.

Tetrayne **1k**

For ferrocenyl-substituted **1k**, an exotherm is found at ~187 °C in the DSC analysis, and a shoulder peak is also noticeable at slightly lower temperature (165 °C; see the Supplementary data). Compound **1k** is remarkably crystalline, and orange-brown translucent needle-shaped crystals of **1k** suitable for X-ray crystallography are obtained easily by diffusion of methanol into an Et_2O solution at -4 °C. The solid-state structure shows that the 16-carbon C_{2v} symmetrical enyne skeleton is virtually planar with a maximum deviation

of 0.056(3) Å from a least-squares plane (Fig. 5). All triple bonds are comparable to other reported tetraynes (Table 3).¹³ The carbons of the tetrayne framework show a gradual curvature with bond angles deviating from 180° by less than 4° in all cases (Table 4). The plane of the cyclopentadienyl ligand for the ferrocene group is, nevertheless, twisted out of the enyne plane by an angle of ~31°.

The most notable feature of the solid-state structure of **1k** is the parallel stacking of tetrayne moieties, suggesting the possibility of a topochemical polymerization. In the solid-state packing of **1k**, molecules show a tilt angle (θ) of 30° and the translational distance (d) is 7.4 Å. There are two potential modes for 1,6-polymerization, with $R_{1,6} = R_{3,8} = 3.7$ Å. Thus, these features correspond quite well with the optimal parameters of $\theta = 28^\circ$, $R_{1,6} < 4$ Å, and $d = 7.4$ Å for topochemical polymerization in a 1,6-addition manner.

With a viable crystal seemingly in hand for effecting 1,6-polymerization, several approaches have been explored. Polymerization via UV irradiation (monochromatic 280 nm for 12 h) fails to induce polymerization, and crystals show a diffraction pattern identical to the original tetrayne sample. Likewise, γ -ray irradiation (^{60}Co , 54 ± 3 krad/h for 2 weeks) also fails to initiate polymerization. Attempts to induce a thermal reaction show that when heated to 150 °C for 30 min, crystals of **1k** transform into a black solid, suggesting that topochemical polymerization of **1k** can be effected through heating. The resulting solid is, however, amorphous rather than crystalline, as established by X-ray crystallographic analysis.

UV-vis spectroscopy was used to analyze the thermal polymerization of **1k** in a solid film cast onto a quartz plate. Three characteristic absorptions are observed for **1k** at 354, 381, and 414 nm, and these absorptions are redshifted by 5–7 nm for **1k** versus those measured in CHCl_3 (Fig. 6). After heating the sample open to air at 150 °C for 5 min, the UV-vis spectrum clearly shows loss of the low-energy absorptions ascribed to the ene-tetrayne-ene moiety, and these signals are replaced by a broad featureless peak at 400–550 nm. Disappointingly, the lack of specific fine structure in the spectrum of the product offers little hint as to the structure(s) resulting from polymerization.

Following the results of the UV-vis study, thermally initiated polymerization of a crystalline sample of **1k** was explored by heating to 150 °C under air. Attempts to analyze the polymerization product by solution-state ^1H and ^{13}C NMR spectroscopy did not, however, afford meaningful spectra because the sample is not soluble in typical organic solvents. Finally, the thermal polymerization for **1k** was monitored by solid-state ^{13}C NMR spectroscopy, while the sample was heated at 150 °C, and spectra were acquired over a period of 5 h (Fig. 7). The solid-state spectrum of the pristine tetrayne **1k** shows excellent resolution in comparison with the solution-state spectrum, and all unique sp and sp^2 carbons of the conjugated skeleton are clearly identified. As the sample is heated, the spectra show gradual peak broadening that increases with heating time. After heating the sample for 300 min, the spectrum is dominated by three broad signals centered at approximately 30, 75, and 142 ppm. The most intense, at δ 75 ppm, seemingly derives from the carbons of the ferrocenyl group (the isotropic ^{13}C chemical shift for solid ferrocene is 70 ppm⁴⁴), and this broad signal engulfs the

Fig. 5. ORTEP drawing (50% probability level) of **1k** showing a segment of crystal packing. Geometry parameters: $\theta = 30^\circ$, $R_{1,6} = 3.7 \text{ \AA}$, $R_{3,8} = 3.7 \text{ \AA}$, and $d = 7.4 \text{ \AA}$. (Note: The numbering of the carbon chain corresponds to the structural characterization listed in Tables 3 and 4, whereas the numbering for $R_{1,6}$ and $R_{3,8}$ refers to reactivity patterns from Fig. 1.)

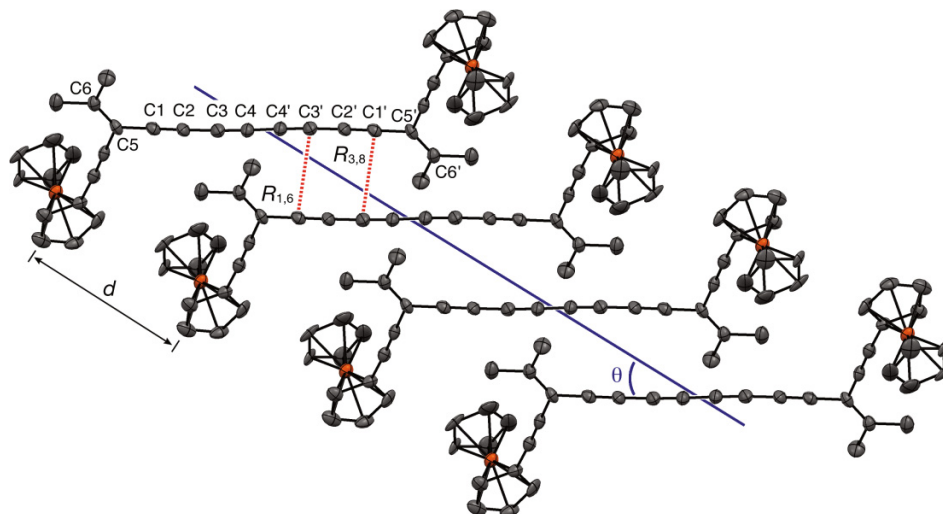


Table 3. Selected bond lengths for tetraynes **1k**, **1l**, **6a**, **6c**, and **6d**.

Product	Bond length (Å)						
	C(1)–C(2)	C(2)–C(3)	C(3)–C(4)	C(4)–C(5)	C(5)–C(6)	C(6)–C(7)	C(7)–C(8)
1k	1.185(5)	1.383(6)	1.211(5)	1.355(8) ^a			
1l	1.200(3)	1.369(3)	1.209(3)	1.365(3)	1.203(3)	1.373(3)	1.200(3)
6a	1.207(4)	1.364(4)	1.199(4)	1.361(5)	1.211(4)	1.357(4)	1.207(4)
6c	1.207(4)	1.365(4)	1.203(4)	1.371(6) ^a			
6d	1.204(4)	1.363(4)	1.204(5)	1.357(7) ^a			

^aC(4)–C(4').

Table 4. Selected bond angles for tetraynes **1k**, **1l**, **6a**, **6c**, and **6d**.

Product	Bond angle (°)									
	C(10)–C(9)–C(1)	C(9)–C(1)–C(2)	C(1)–C(2)–C(3)	C(2)–C(3)–C(4)	C(3)–C(4)–C(5)	C(4)–C(5)–C(6)	C(5)–C(6)–C(7)	C(6)–C(7)–C(8)	C(7)–C(8)–C(11)	C(8)–C(11)–C(12)
1k	121.3(4) ^a	178.9(5) ^b	176.6(5)	177.1(5)	177.5(6) ^c					
1l	121.95(18)	179.1(2)	177.8(2)	177.5(2)	179.4(2)	179.5(3)	178.1(2)	177.1(2)	178.2(2)	121.22(18)
6a	119.5(3)	177.4(4)	179.0(4)	179.4(4)	179.3(4)	179.8(4)	179.7(4)	177.8(4)	176.8(4)	118.3(3)
6c	120.9(3) ^a	175.9(3) ^b	178.3(3)	178.5(3)	179.6(4) ^c					
6d	120.2(3) ^a	174.3(4) ^b	179.1(4)	177.1(4)	179.8(6) ^c					

^aC(6)–C(5)–C(1).

^bC(5)–C(1)–C(2).

^cC(3)–C(4)–C(4').

region where polyynes signals are expected, making any particular assignments impossible. The signal at the highest chemical shift is very broad, spanning from 120–160 ppm, and probably results from sp^2 carbons of the vinylidene carbons and olefinic carbons formed during polymerization, or both. A background signal from the probe is also expected to contribute signal to this region. Thus, in comparison with **1j**, there is little clear evidence that **1k** polymerizes through a regioselective process, i.e., 1,6-addition, as suggested by its crystallographic analysis.

Tetrayne **1l**

DSC analysis of crystalline **1l** shows a well-defined melting point at 103–104 °C, which is then followed by decomposition of the sample at 145 °C (see the Supplementary data). Yellow single crystals of tetrayne **1l** are obtained by diffusion of MeOH into a CH_2Cl_2 solution at –20 °C. Surprisingly, two different polymorphs of **1l** could be obtained from seemingly identical crystallization conditions. In addition, there appears to be no way to direct which polymorph will result for a given crystallization attempt. Both solid-state structures adopt geo-

Fig. 6. Solid-state UV–vis spectra for **1k** before and after heating the thin-film sample to 150 °C for 5 min.

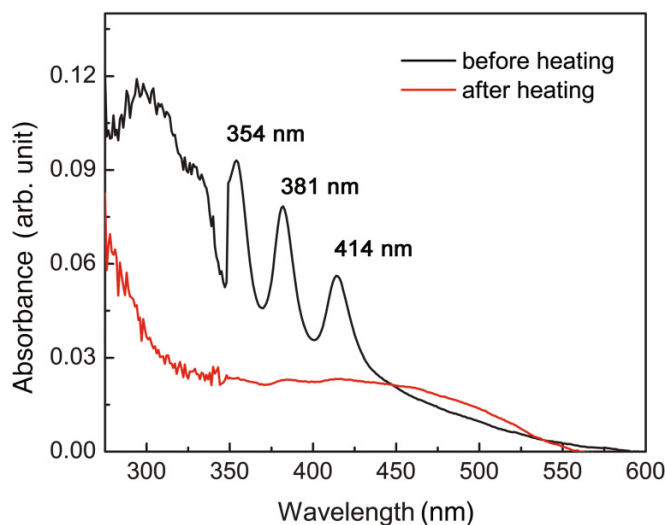
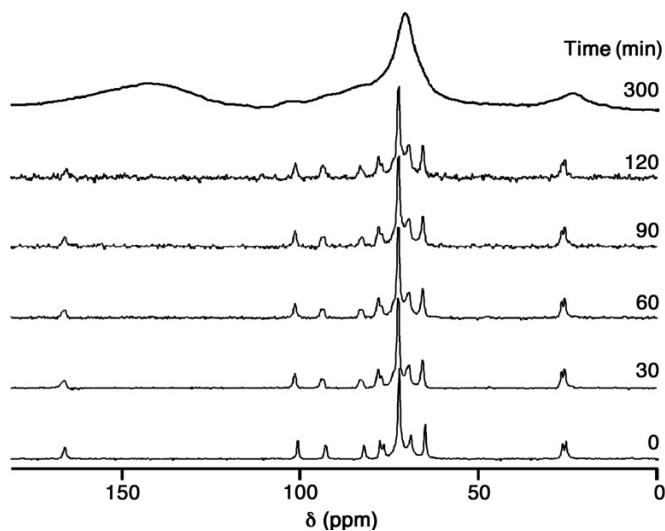


Fig. 7. Solid-state ^{13}C NMR spectra for **1k** recorded before and after heating at 150 °C for the times shown.



metrically similar s-trans orientations with respect to the octatetrayndiyl moiety (as shown in Fig. 8).²⁷ For one structure, molecules are aligned in parallel stacks, such that topochemical polymerization might be possible (this structure is shown in Fig. 8). The π framework of **11** in this polymorph is virtually planar, with a maximum deviation of 0.02 Å from a least-squares plane for the 16 carbons of the conjugated skeletons. Triple bonds are unremarkable and comparable to other reported polyynes of this length (Table 3).^{13,45} The eight tetrayne carbons show only a slight curvature with bond angles deviating from linear by less than 3° in all cases (Table 4).

Crystal packing analysis of tetrayne **11** shows that the individual molecules are aligned in a parallel fashion that is predicted to favour the 1,6-addition polymerization (Fig. 8). The packing parameters of $\theta = 28^\circ$ and $d = 7.7$ Å correspond quite well to those required for 1,6-polymerization, while two

close contacts are also in a favourable range, $R_{1,6} = 3.7$ Å and $R_{3,8} = 3.6$ Å.

In spite of the favourable packing parameters observed for **11**, all efforts to effect the thermal polymerization of single crystals for this tetrayne have been unsuccessful. Heating a sample of **11** at 90 °C (i.e., just below the melting point) for 8 h gives a sample that is slightly darkened to yield an opaque solid that is no longer crystalline as documented by the absence of an X-ray diffraction pattern. Other methods to initiate the polymerization have also been explored, including monochromatic UV irradiation (280 nm for 24 h) and γ -irradiation (54 ± 3 krad/h for 2 weeks). In both cases, darkened yellow-orange single crystals are produced. X-ray analysis of these crystals, however, reveals exactly the same diffraction pattern as found for pristine **11**, and there appears to be little change in the solid beyond a possible reaction at the outer surface of the crystal. Thus, there is so far no efficient way to trigger a solid-state polymerization in single crystals of **11**.

Tetrayne 6a

DSC analysis of tetrayne derivative **6a** shows a sharp, narrow exotherm at 192 °C, which is consistent with the possibility of a reasonably well-defined topochemical polymerization (see the Supplementary data). Compound **6a** affords crystals for X-ray crystallography from a mixture of hexanes and CH_2Cl_2 . The solid-state structure (Fig. 9 and Tables 3 and 4) shows that neighbouring molecules align in stacks as centrosymmetric dimeric pairs, thus giving an alternating A–B–A–B pattern. This is most easily identified in Fig. 9 by the different twist angles of the phenyl rings, which rotate out of the planar enyne framework by $\sim 56^\circ$ and 43° . The C–C \equiv C angles of **6a** deviate slightly from linearity, but by no more than about 3° (Table 4), whereas the torsion angle generated from vinyl groups (C10–C9...C11–C12) is $\sim 3^\circ$.

Analysis of the solid-state packing parameters shows that the tetrayne groups of neighbouring molecules are aligned with $\theta = 42^\circ$, $R_{1,4} = R_{3,6} = R_{5,8} = 3.4$ Å, and $d = 5.1$ Å. Thus, whereas 1,6-polymerization is not possible ($R_{1,6} = 4.3$ Å), the observed packing values are quite close to the optimal values for 1,4-polymerization ($\theta = 45^\circ$, $R_{1,4} < 4$ Å, and $d = 5.1$ Å). Combined with the intense and sharp exotherm in the DSC measurement, it seems possible that compound **6a** might undergo a 1,4-topochemical polymerization reaction. Because of our focus on 1,6-polymerization processes, however, further studies on **6a** have not yet been conducted.

Tetrayne 6b

The DSC spectrum of tetrayne **6b** shows a sharp endotherm at ~ 176 °C, immediately followed by a broad exotherm at 179 °C (see the Supplementary data). No melting point is, however, observed in a capillary melting point analysis. Thus, it is not clear if the initial endotherm observed by DSC is a phase transition or a true melting point. In any case, this behaviour suggests that product analysis from a thermal solid-state reaction would not be straightforward, so no further analysis of this compound has been pursued.

Tetrayne 6c

Compound **6c** shows an apparent melting point of 168–170 °C in a capillary melting point analysis, and the sample slowly darkens as the temperature is increased. DSC analysis,

Fig. 8. ORTEP drawing (50% probability level) of **11** showing a segment of crystal packing. Geometry parameters: $\theta = 28^\circ$, $R_{1,6} = 3.7 \text{ \AA}$, $R_{3,8} = 3.6 \text{ \AA}$, and $d = 7.7 \text{ \AA}$. (Note: The numbering of the carbon chain corresponds to the structural characterization listed in Tables 3 and 4, whereas the numbering for $R_{1,6}$ and $R_{3,8}$ refers to reactivity patterns from Fig. 1.)

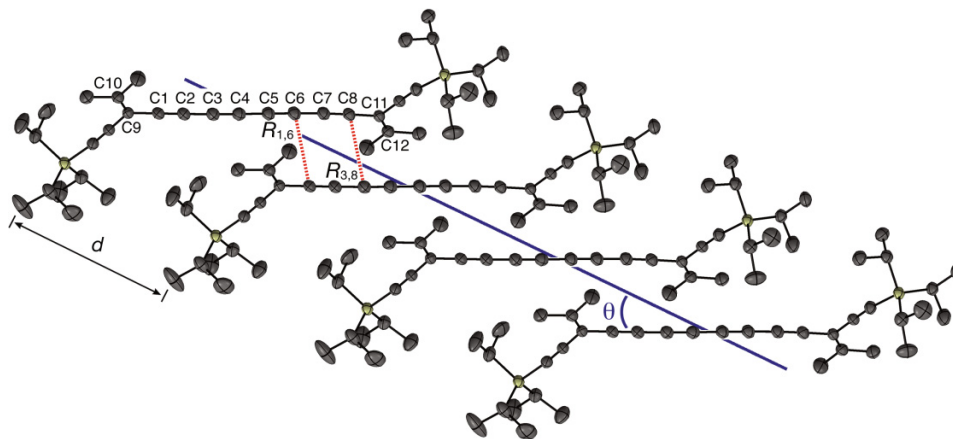
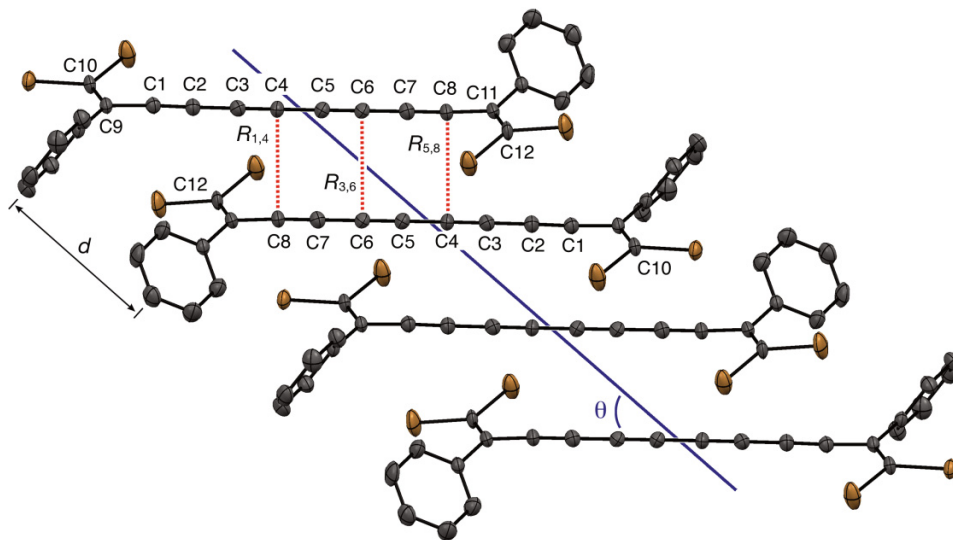


Fig. 9. ORTEP drawing (50% probability level) of **6a** showing a segment of the crystal packing. Geometry parameters: $\theta = 42^\circ$, $R_{1,4} = 3.4 \text{ \AA}$, $R_{3,6} = 3.4 \text{ \AA}$, $R_{5,8} = 3.4 \text{ \AA}$, and $d = 5.1 \text{ \AA}$. (Note: The numbering of the carbon chain corresponds to the structural characterization listed in Tables 3 and 4, whereas the numbering for $R_{1,4}$, $R_{3,6}$, and $R_{5,8}$ refers to reactivity patterns from Fig. 1.)



on the other hand, shows an initial broad, weak exotherm with an onset at about 190°C , and a second, sharp exotherm that initiates at about 230°C , with a maximum at 233°C (see the Supplementary data).

X-ray quality crystals of **6c** were obtained via the diffusion of hexanes into a solution of **6c** in hexanes/ CH_2Cl_2 at -4°C . The solid-state structure of **6c** (Fig. 10 and Tables 3 and 4) reveals that the terminal acetylene angles $\text{C}(5)\text{--}\text{C}(1)\text{--}\text{C}(2)$ are the most distorted at $175.9(3)^\circ$. The enyne framework of the centrosymmetric structure is completely planar, whereas the aryl rings twist significantly from this plane by 65° . Analysis of the crystal packing shows that neighbouring molecules of compound **6c** are aligned in a parallel fashion, and the packing parameters for **6c** are similar to that observed for **6a**, with $\theta = 38^\circ$, $R_{1,4} = 3.8 \text{ \AA}$, $R_{3,6} = 3.7 \text{ \AA}$, $R_{5,8} = 3.8 \text{ \AA}$, and $d = 5.9 \text{ \AA}$. Thus, packing parameters are suboptimal for either 1,4- or

1,6-polymerization, and thermal analysis of this compound has not been further explored.

Tetrayne **6d**

DSC analysis of the nitro-derivative **6d** shows a very sharp exotherm at 191°C ($T_{\text{onset}} = 189^\circ\text{C}$ and $T_{\text{max}} = 191^\circ\text{C}$, see the Supplementary data). **Warning:** An explosion occurred at approximately 190°C when heating a small quantity of compound **6d** (60 mg) in a capped tightly packed solid-state NMR rotor. When handling any polyyne, one should always take the appropriate safety precautions when the sample is heated above room temperature. This is particularly true if the sample is a terminal polyyne, where precautions should be taken at all temperatures.

Single crystals of **6d** for analysis by X-ray crystallography were obtained via the evaporation of a CDCl_3 or CHCl_3

Fig. 10. ORTEP drawing (50% probability level) of **6c** showing a segment of the crystal packing. Geometry parameters: $\theta = 38^\circ$, $R_{1,4} = 3.8 \text{ \AA}$, $R_{3,6} = 3.7 \text{ \AA}$, $R_{5,8} = 3.8 \text{ \AA}$, and $d = 5.9 \text{ \AA}$. (Note: The numbering of the carbon chain corresponds to the structural characterization listed in Tables 3 and 4, whereas the numbering for $R_{1,4}$, $R_{3,6}$, and $R_{5,8}$ refers to reactivity patterns from Fig. 1.)

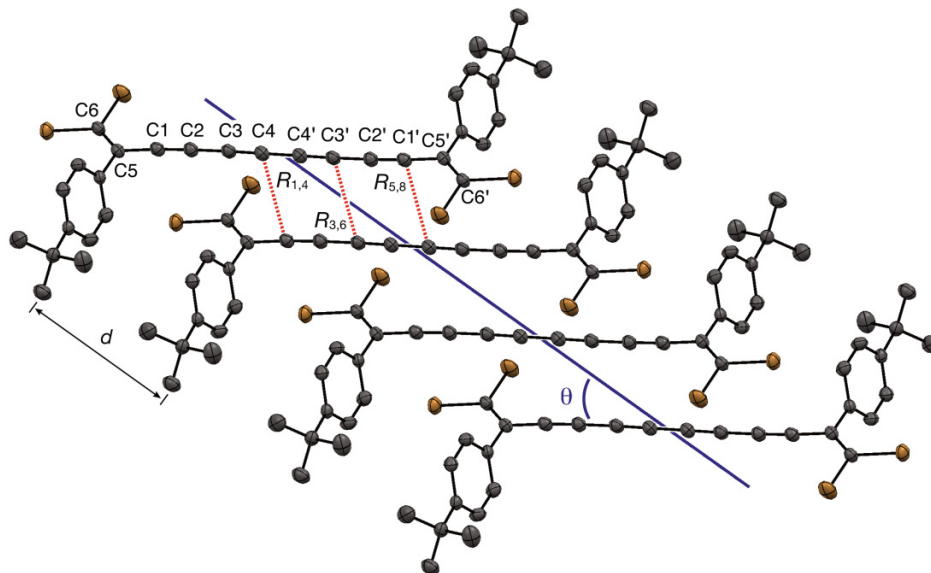
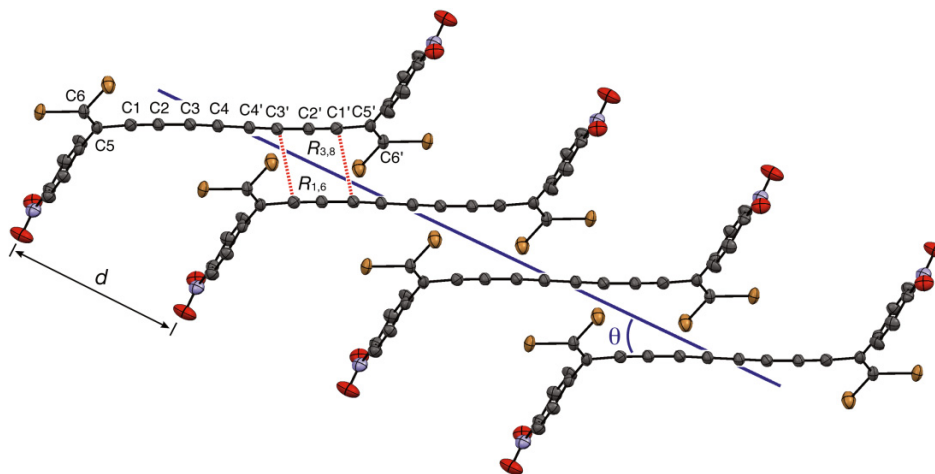


Fig. 11. ORTEP drawing (50% probability level) of **6d** showing a segment of crystal packing. Geometry parameters: $\theta = 29^\circ$, $R_{1,6} = 3.5 \text{ \AA}$, $R_{3,8} = 3.5 \text{ \AA}$, and $d = 7.5 \text{ \AA}$. (Note: The numbering of the carbon chain corresponds to the structural characterization listed in Tables 3 and 4, whereas the numbering for $R_{1,6}$ and $R_{3,8}$ refers to reactivity patterns from Fig. 1.)



solution at -4°C (Fig. 11). As with **6a** and **6c** (Table 4), the terminal C(5)–C(1)–C(2) bond angle of **6d** is the most distorted from linearity at $174.3(4)^\circ$, and the centrosymmetric enyne framework is planar. Molecules of compound **6d** are packed in parallel stacks, and the distance separating reactive atoms of adjacent molecules is $R_{1,6} = R_{3,8} = 3.5 \text{ \AA}$. The translational distance (d) is 7.5 \AA , with a packing angle (θ) of 29° . These values are thus ideal for a 1,6-topochemical polymerization.

The UV–vis absorption spectrum of compound **6d** has been measured in the solid state (Fig. 12) for a thin film produced by casting a solution of compound **6d** in CH_2Cl_2 onto a quartz slide and allowing the solvent to evaporate. The UV–vis spectrum of the film shows absorbance values of 368, 400, and 434 nm, which

are somewhat red-shifted from those for the sample in solution (359, 384, and 419 nm in THF). As the thin film is then heated at 170°C under an argon atmosphere for 17 h, UV–vis absorption spectra have been examined at various time intervals (Fig. 12). After heating for 1 h, the intensity of the three low-energy absorbances decreases, and λ_{max} values are slightly blue-shifted to 365, 397, and 430 nm. After heating for 5 h, only two distinct signals remain in the low-energy region at ~ 393 and 424 nm, and these two signals finally merge into one broad signal after heating for a total of 17 h. Rather surprisingly, this analysis implies that the conjugated ene–tetrayne–ene framework is transformed into a *less conjugated* product, rather than one with extended conjugation as would be expected upon formation of a polytriacetylene product (Fig. 13).

Fig. 12. Solid-state UV-vis spectra for compound **6d** before and after heating at 170 °C for the times given.

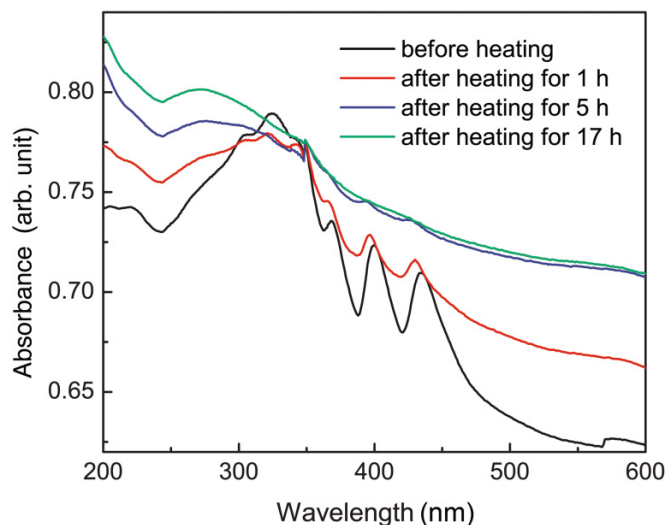
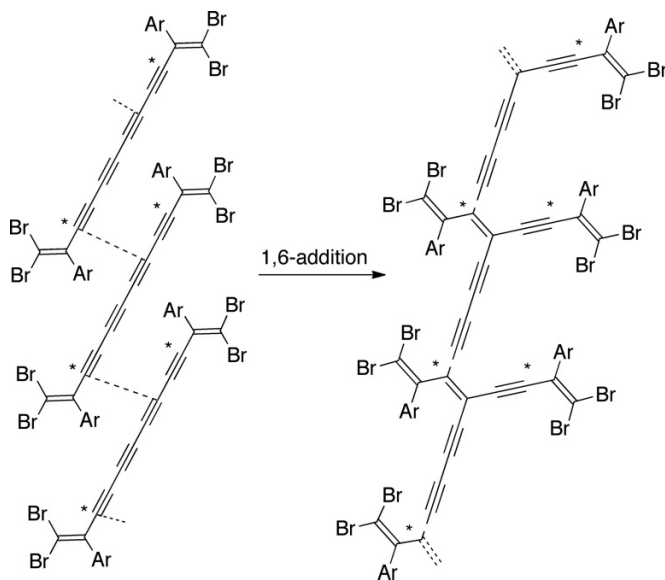
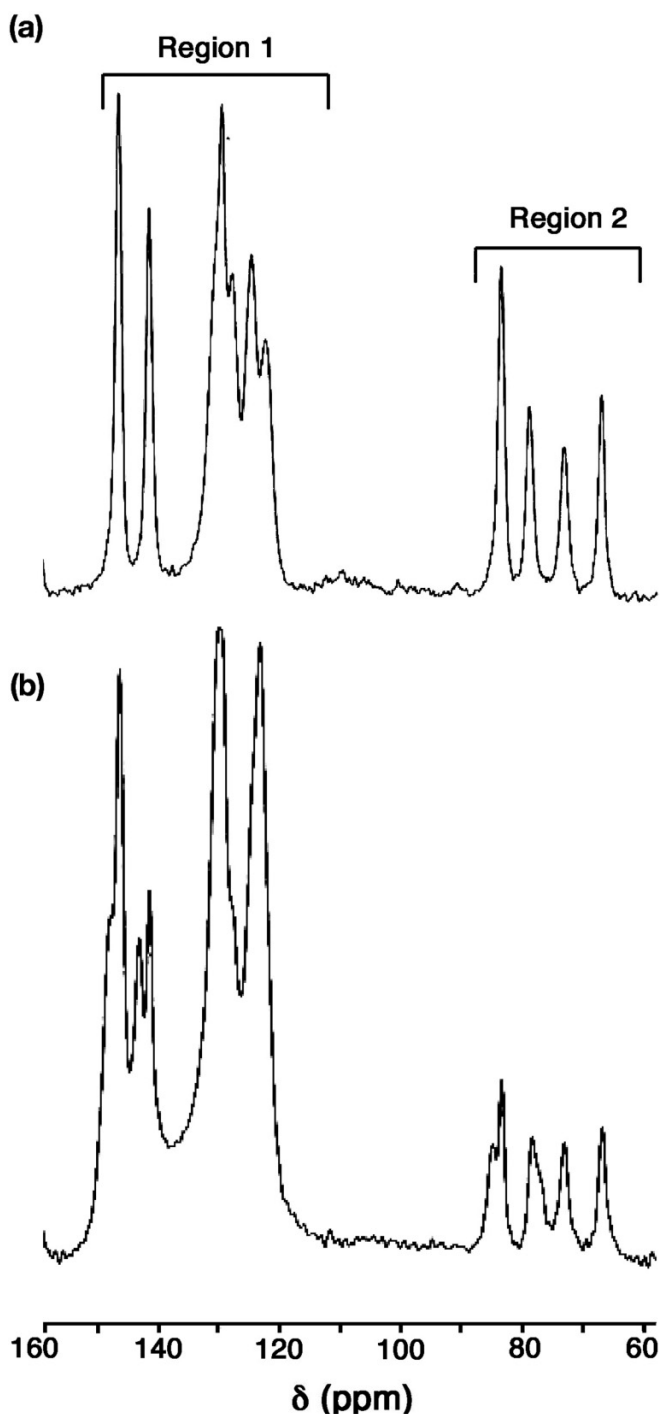


Fig. 13. Idealized structure resulting from 1,6-polymerization of **6d** or labeled **6d/6d*/6d**** (* indicates ^{13}C atoms).



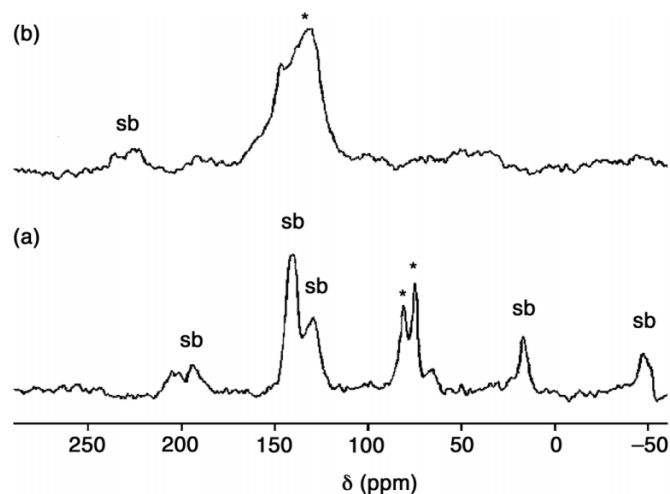
Thermal polymerization of **6d** has been explored by heating a crystalline sample to 170 °C under argon (see the previous warning for compound **6d**). Attempts to analyze the resulting sample by solution-state ^1H and ^{13}C NMR spectroscopy show that the resulting polymer is insoluble, and useful spectra could not be obtained. Solid-state ^{13}C NMR spectroscopy has therefore been used to explore the thermal transformation of **6d** (Fig. 14). In the pristine sample, four aromatic and two alkenyl signals are observed in region 1 (Fig. 14, 120–150 ppm). These resonances are found at similar chemical shifts as in solution, except for the α -vinyl signal ($\text{Br}_2\text{C}=\text{C}<$), which appears downfield from its solution value of 107.5 ppm. The alkynyl peaks appear in region 2 (Fig. 14, 60–90 ppm), and chemical shifts for the four distinct signals (67, 73, 79, and 84 ppm) correlate well with those found in the solution-state

Fig. 14. Solid-state ^{13}C NMR spectra of compound **6d** (a) before heating and (b) after heating at 170 °C for 6 h under argon.



spectrum at 64.8, 71.2, 75.9, and 82.6 ppm. After heating the solid at 170 °C under an Ar atmosphere for 6 h, both downfield signals in region 1 (Fig. 14, 142 and 147 ppm) appear to split into two signals, while the remaining two signals in region 1 broaden somewhat. Signals in region 2 follow a similar pattern, where two signals (79 and 84 ppm) seemingly split and those at 67 and 73 ppm broaden slightly. Furthermore, the intensity of all alkyne signals in region 2 decreases noticeably

Fig. 15. Solid-state ^{13}C NMR spectra for compound **6d/6d*/6d****. (a) Before heating. (b) After heating (sb, spinning side band; *, labelled ^{13}C signal). Spectra were acquired at 11.75 T (125 MHz for ^{13}C) using CP/MAS and a spinning frequency of 8 kHz. Spectra acquired at various spinning frequencies (not shown) confirmed that the peaks in the 100–150 ppm region in (a) arise primarily from spinning sidebands.



relative to those in region 1. The spectral changes in regions 1 and 2 for the spectrum acquired after heating suggest a loss of molecular symmetry, which is evidence for polymerization as shown for the idealized transformation outlined in Fig. 13. Unfortunately, it is once again not clear if the reaction proceeds via a 1,6-addition process as suggested by X-ray crystallographic analysis or via an alternative pathway.

Crystals of partially labelled tetrayne sample **6d/6d*/6d**** could be obtained, but unfortunately only on a small scale, giving a total sample amount of ~1 mg. X-ray crystallography has established that the solid-state geometric packing of this sample is identical to that of unlabelled **6d**. A solid-state ^{13}C NMR spectrum of **6d/6d*/6d**** was acquired at 11.75 T (125 MHz for ^{13}C) using cross-polarization/magic-angle spinning (CP/MAS) and a spinning frequency of 8 kHz (Fig. 15). In the pristine sample, two strong signals are observed at 75.4 and 81.5 ppm owing to the presence of ^{13}C labelling. This is surprising given that the solid-state structure of **6d** is expected to be centrosymmetric based on the crystallographic analysis, and only a single resonance for the labelled carbon is observed in solution (75.6 ppm; see the Supplementary data). The origin of the second signal is, at present, unexplained. Unfortunately, spinning side bands are also quite intense. After heating the sample holder containing compound **6d/6d*/6d**** at 170 °C under Ar for 3 days, the resulting spectrum shows the enhanced ^{13}C signals at ~130 and 142 ppm, characteristic of sp^2 -hybridized carbon atoms. At first sight, this result is inconsistent with the analysis of unlabelled **6d** for which alkyne signals are still observed after heating (Fig. 14). It is likely, however, that the extended heating time for **6d/6d*/6d**** at 170 °C (3 days) versus that of **6d** (6 h) results in additional and nonselective reactions, ultimately giving a material composed primarily of sp^2 -hybridized carbon. Thus, compound **6d/6d*/6d**** may undergo a 1,6-topochemical polymerization, but the structure of the final product, frustratingly, remains unsolved.

Conclusions

We have described the synthesis of functionalized, cross-conjugated tetraynes. UV–vis spectroscopic analysis shows that the electronic characteristics of the tetrayne moiety dominate the lower energy absorption region, and the side groups, either electron-donating or electron-withdrawing, have only a marginal influence on the absorption energy of the central tetrayne chromophore. The solid-state structural properties of five derivatives have been examined by X-ray crystallographic analysis. Examination of the crystal structures with an eye toward inducing solid-state reactions shows that the packing parameters (θ , R , and d) for all but **6c** fall within a range suitable for topochemical polymerization, and the values for three (**1k**, **1l**, and **6d**) are quite close to the values ideal for a 1,6-polymerization. To our knowledge, this is the first series of structurally similar tetraynes that shows a consistent packing motif conducive to topochemical polymerization. In addition to X-ray crystallography, DSC analysis also supports the prospect of a viable polymerization reaction toward a defined product in many cases. Thus, the polymerization of tetraynes has been explored using thermal, photochemical, and (or) γ -irradiation for initiation. Furthermore, the thermally induced solid-state reaction of **1d**, **1j**, **1k**, and **6d** has been studied in more detail via solid-state ^{13}C NMR spectroscopy. In all cases, however, it has been frustratingly difficult to ascertain the structure of the product, often owing to broadening of the observed resonances in the ^{13}C spectra, presumably because of a regiorandom polymerization reaction.

Our inability to effect clean polymerization of these crystallized samples is the most significant outcome of this study. A survey of reports for topochemical polymerization of diynes shows that there is typically a good correlation between packing parameters and successful polymerization to a polydiacetylene product. Combined with reports of successful polymerization of polyynes as described in the Introduction, this leads to the naïve assumption that the controlled polymerization of polyynes might also be predicted based on solid-state packing. But the story is not so simple, and it is now quite obvious to conclude that the successful polymerization of tetraynes is far more complex than a simple analysis of solid-state packing parameters θ , R , and d .

Experimental section

Irradiation with ^{60}Co

Single crystals of either **4k** or **4l** were placed into a glass vial and subjected to the irradiation from a ^{60}Co source ($\sim 54 \pm 3$ krad/h, previously located at the Chemistry Department, University of Alberta, Edmonton, Alberta) for 2 weeks at room temperature. After irradiation, the colours of the crystals became slightly darker and the crystals were re-examined by X-ray single crystal diffraction analysis.

X-ray crystallographic data

Data for **1k**

Single crystals of **1k** were obtained via the diffusion of methanol into an Et_2O solution at -4 °C. Formula $\text{C}_{40}\text{H}_{30}\text{Fe}_2$, fw = 622.34; monoclinic crystal system, space group $P2_1/c$ (No. 14); $a = 18.075(3)$ Å, $b = 7.4082(11)$ Å, $c = 11.7293(16)$ Å; $\beta = 103.751(3)^\circ$; $V = 1525.6(4)$ Å³; $Z = 2$; $\rho_{\text{calcd.}} = 1.355$ g cm⁻³; $2\theta_{\text{max}} = 52.80^\circ$; $\mu = 0.978$ mm⁻¹;

$T = -80\text{ }^{\circ}\text{C}$; total data collected = 7305. Final $R_1(F) = 0.0562$ (1455 observed reflections with $F_o^2 \geq 2\sigma(F_o^2)$); $wR_2(F^2) = 0.0901$ for 212 variables, 3133 unique reflections, and 0 restraints; residual electron density = 0.326 and $-0.327\text{ e } \text{\AA}^{-3}$. CCDC 862755.

Data for 11

Single crystals of **11** were obtained via the diffusion of MeOH into a CH_2Cl_2 solution at $-20\text{ }^{\circ}\text{C}$ (as reported in ref. 27). Formula $\text{C}_{38}\text{H}_{54}\text{Si}_2$, fw = 566.99; monoclinic crystal system, space group $P2_1/c$ (No. 14); $a = 13.5571(8)\text{ \AA}$, $b = 7.7132(5)\text{ \AA}$, $c = 35.616(2)\text{ \AA}$; $\beta = 96.5990(10)^{\circ}$; $V = 3699.7(4)\text{ \AA}^3$; $Z = 4$; $\rho_{(\text{calcd.})} = 1.018\text{ g cm}^{-3}$; $2\theta_{\text{max}} = 51.50^{\circ}$; $\mu = 0.118\text{ mm}^{-1}$; $T = -80\text{ }^{\circ}\text{C}$; total data collected = 19122. Final $R_1(F) = 0.0472$ (4842 observed reflections with $F_o^2 \geq 2\sigma(F_o^2)$); $wR_2(F^2) = 0.1366$ for 365 variables, 7039 unique reflections, and 0 restraints; residual electron density = 0.389 and $-0.235\text{ e } \text{\AA}^{-3}$. CCDC HOZSAQ.

Data for 6a

Single crystals of **6a** were obtained via the diffusion of hexanes into a solution of hexanes/ CH_2Cl_2 at $-4\text{ }^{\circ}\text{C}$. Formula $\text{C}_{24}\text{H}_{10}\text{Br}_4$, fw = 617.96; triclinic crystal system, space group $P\bar{1}$ (No. 2); $a = 9.4512(7)\text{ \AA}$, $b = 10.1187(7)\text{ \AA}$, $c = 11.6133(8)\text{ \AA}$; $\alpha = 96.0941(13)^{\circ}$, $\beta = 92.5663(13)^{\circ}$, $\gamma = 103.4569(13)^{\circ}$; $V = 1071.25(13)\text{ \AA}^3$; $Z = 2$; $\rho_{(\text{calcd.})} = 1.916\text{ g cm}^{-3}$; $2\theta_{\text{max}} = 52.76^{\circ}$; $\mu = 7.521\text{ mm}^{-1}$; $T = -80\text{ }^{\circ}\text{C}$; total data collected = 7878. $R_1 = 0.0368$ (3413 observed reflections with $F_o^2 \geq 2\sigma(F_o^2)$); $wR_2 = 0.0930$ for 253 variables, 4356 unique reflections, and 0 restraints; residual electron density = 1.164 and $-0.586\text{ e } \text{\AA}^{-3}$. CCDC 862756.

Data for 6c

Single crystals of **6c** were obtained via the diffusion of hexanes into a solution of hexanes/ CH_2Cl_2 at $-4\text{ }^{\circ}\text{C}$. Formula $\text{C}_{32}\text{H}_{26}\text{Br}_4$, fw = 730.17; triclinic crystal system, space group $P\bar{1}$ (No. 2); $a = 5.8968(7)\text{ \AA}$, $b = 11.1037(14)\text{ \AA}$, $c = 11.9247(15)\text{ \AA}$; $\alpha = 69.2510(17)^{\circ}$, $\beta = 78.1507(18)^{\circ}$, $\gamma = 86.0880(19)^{\circ}$; $V = 714.58(15)\text{ \AA}^3$; $Z = 1$; $\rho_{(\text{calcd.})} = 1.697\text{ g cm}^{-3}$; $2\theta_{\text{max}} = 52.74^{\circ}$; $\mu = 5.651\text{ mm}^{-1}$; $T = -80\text{ }^{\circ}\text{C}$; total data collected = 5606. $R_1 = 0.0342$ (2418 observed reflections with $F_o^2 \geq 2\sigma(F_o^2)$); $wR_2 = 0.0905$ for 163 variables, 2911 unique reflections, and 0 restraints; residual electron density = 0.618 and $-0.492\text{ e } \text{\AA}^{-3}$. CCDC 862758.

Data for 6d

Single crystals of **6c** were obtained via the evaporation of a CDCl_3 solution at $-4\text{ }^{\circ}\text{C}$. Formula $\text{C}_{24}\text{H}_8\text{Br}_4\text{N}_2\text{O}_4$, fw = 707.96; orthorhombic crystal system, space group $Pbcn$ (No. 60); $a = 7.5156(7)\text{ \AA}$, $b = 14.8934(14)\text{ \AA}$, $c = 21.328(2)\text{ \AA}$; $V = 2387.3(4)\text{ \AA}^3$; $Z = 4$; $\rho_{(\text{calcd.})} = 1.970\text{ g cm}^{-3}$; $2\theta_{\text{max}} = 52.82^{\circ}$; $\mu = 6.777\text{ mm}^{-1}$; $T = -80\text{ }^{\circ}\text{C}$; total data collected = 14313. $R_1 = 0.0322$ (1968 observed reflections with $F_o^2 \geq 2\sigma(F_o^2)$); $wR_2 = 0.0825$ for 154 variables, 2461 unique reflections, and 0 restraints; residual electron density = 1.129 and $-0.406\text{ e } \text{\AA}^{-3}$. CCDC 862757.

Synthetic and spectroscopic details

General experimental details

Column chromatography: silica gel 60 (230–400 mesh) from General Intermediates of Canada. Thin-layer chromatog-

raphy (TLC): aluminium sheet coated with silica gel F_{254} from Whatman; visualization by UV light or KMnO_4 stain. Melting point: Fisher-Johns or Gallenkamp apparatus; uncorrected. UV-vis spectra: Varian Cary 400 at rt; λ in nm (ϵ in $\text{L mol}^{-1}\text{ cm}^{-1}$). IR spectra (cm^{-1}): Nicolet Magna-IR 750 (neat) or Nic-Plan IR microscope (solids). ^1H and ^{13}C solution-state NMR: Varian 300, 400, 500, or 600 and Bruker AM-300 instruments, at rt in CDCl_3 ; solvent peaks (7.24 ppm for ^1H and 77.0 ppm for ^{13}C) as reference. For simplicity, the coupling constants of the aryl protons have been reported as pseudo-first-order, even though they are AA'BB' second-order spin systems; coupling constants are reported as observed. ^{13}C solid-state NMR: CMX Infinity 200 as well as Bruker Avance 300 and 500 spectrometers operating at 50, 75, and 125 MHz, respectively, for ^{13}C . Samples were packed in 4 mm outside diameter (o.d.) MAS rotors spinning at frequencies ranging from 5 to 12 kHz. All spectra were acquired with cross polarization using contact times of 1.0–6.0 ms, ^1H 90° pulses of 2.5–4.0 μs , and recycle delays of 3.0–10.0 s. To improve decoupling efficiency, the two-pulse phase modulated (TPPM) sequence of Griffin and co-workers⁴⁶ was used. Spectra were referenced to tetramethylsilane (TMS; $\delta = 0$) by setting the high-frequency peak of adamantane to 38.56 ppm.⁴⁷ EI-MS (m/z): Kratos MS 50 instrument. ESI-MS (m/z): Micromass Zabspec oaTOF or PE Biosystems Mariner TOF instruments. Elemental analyses were performed by the Microanalytical Service, Department of Chemistry, University of Alberta.

General methods

Reagents and solvents were purchased reagent grade and used without further purification. Compounds **2**,²⁹ **3b**,⁴⁸ **3g**,⁴⁹ **3k**,⁵⁰ **10a–10c**,³¹ and **11**³⁵ were prepared based on literature precedent. Anhydrous MgSO_4 was used as the drying agent after aqueous workup. Evaporation and concentration in vacuo was done at H_2O -aspirator pressure. All reactions were performed in standard glassware under an inert atmosphere of Ar or N_2 . A positive pressure of Ar or N_2 was essential to the success of all Pd-catalyzed reactions. Deoxygenation of solvents was accomplished by vigorously bubbling Ar or N_2 through the solution at rt for ~30 min. Brine refers to a saturated aqueous solution of NaCl. Flash chromatography was conducted on silica gel using the eluent system defined in the individual experimental procedures.

For mass spectrometric analyses, low-resolution data are provided in cases when M^+ is not the base peak; otherwise, only high-resolution data are provided. The samples for ESI mass spectrometry were typically dissolved in $\text{ClCH}_2\text{CH}_2\text{Cl}$ and made use of a 3:1 MeOH/toluene mixture as the carrier solvent.

DSC measurements were measured on a PerkinElmer Pyris 1 DSC instrument. Melting points from DSC analysis are reported as the peak maxima, and in cases when the sample decomposed, the onset temperature of the decomposition exothermic peak is reported, as well as the exothermic maxima corresponding to the decomposition.

Formation of the Hay catalyst was conducted as follows: CuI (50 mg) and tetramethylethylenediamine (TMEDA, 75 mg) were added to CH_2Cl_2 (2 mL) and stirred until homogeneous; this solution was prepared fresh for each reaction. Wet THF/MeOH refers to the use of THF and MeOH that have not been previously dried by distillation, i.e., the solvent is

used “straight out of the bottle” and is assumed to contain a small amount of water.

General procedure A — Desilylation procedure

To the appropriate trimethylsilyl polyene in wet THF/MeOH (1:1, 20 mL) was added K_2CO_3 (~20 mg), and the resulting mixture was stirred at rt until TLC indicated the starting material had been consumed (~2 h). Ether (50 mL) and saturated aq NH_4Cl (50 mL) were added, the organic phase separated, washed with saturated aq NH_4Cl (2×50 mL), dried over $MgSO_4$, and filtered. The solvent was then reduced to ~1 mL via rotary evaporation, taking care to ensure that the product remained in solution during the concentration process. The resulting solution was carried on to the next step.

General procedure B — Palladium-catalyzed cross-coupling procedure

The appropriate alkyne **3** was added to a solution of vinyl triflate **2** in THF (20 mL) and the resulting mixture deoxygenated. $PdCl_2(PPh_3)_2$ (~0.05 equiv) and *i*- Pr_2NH were sequentially added, the solution was stirred for 5 min, CuI (~0.15 equiv) was added, and the solution was stirred under conditions described in the individual procedures, typically until TLC analysis no longer showed the presence of either **2** or **3**. Ether (40 mL) and H_2O (30 mL) were then added, the organic phase separated, washed with saturated aq NH_4Cl (2×50 mL), dried over $MgSO_4$, filtered, and the filtrate concentrated in vacuo. Flash column chromatography and (or) precipitation from MeOH gave the desired enyne oligomer.

General procedure C — Copper-catalyzed oxidative acetylenic-coupling procedure

The terminal acetylene from general procedure A was added to acetone (10 mL), acetone/ CH_2Cl_2 (1:1, 10 mL), or CH_2Cl_2 (60 mL). A solution of Hay catalyst mixture (1 mL) was then added. The mixture was stirred at rt under air until TLC analysis no longer showed the deprotected polyene (generally less than 0.5 h). The reaction solution was concentrated in vacuo to ~5 mL and diethyl ether (50 mL) was added. The ethereal solution was consecutively washed with a 10% HCl solution (25 mL), saturated aq $NaHCO_3$ (25 mL), and brine (25 mL), dried, and the solvent removed. Flash column chromatography and (or) precipitation from MeOH gave the product **1** or **6**.

Compound 1a

Compound **4a** (66 mg, 0.26 mmol) was desilylated with K_2CO_3 in MeOH/THF (1:1) as described in general procedure A, and homocoupled in acetone (10 mL) in the presence of Hay catalyst (1 mL) and air for 1 h as described in general procedure C. Flash chromatography (hexane/ CH_2Cl_2 , 2:1) afforded **1a** (45 mg, 94%) as a brown oil that slowly decomposed over a period of hours to days when stored neat. R_f = 0.78 (hexane/ CH_2Cl_2 , 2:1). UV-vis ($CHCl_3$) λ_{max} (ϵ): 302 (57 800), 320 (41 700), 348 (17 100), 374 (18 800), 405 (11 800). IR ($CHCl_3$, cast, cm^{-1}): 2958, 2932, 2872, 2193, 2125, 1959, 1587. 1H NMR (300 MHz, $CDCl_3$) δ : 2.33 (t, J = 6.6 Hz, 4H), 2.02 (s, 6H), 2.01 (s, 6H), 1.54–1.36 (m, 8H), 0.90 (t, J = 7.2 Hz, 6H). ^{13}C NMR (75 MHz, $CDCl_3$, APT) δ : 159.7, 100.5, 94.2, 75.7, 75.8, 75.5, 67.7, 64.0, 30.8, 23.1, 23.0, 22.0, 19.2, 13.6. EI HR-MS calcd for $C_{28}H_{30}$ (M^+): 366.2347; found: 366.2349.

Compound 1b

Compound **4b** (20 mg, 0.035 mmol) was desilylated with K_2CO_3 in MeOH/THF (1:1) as described in general procedure A, and homocoupled in acetone (10 mL) in the presence of Hay catalyst (1 mL) and air for 0.5 h as described in general procedure C. Flash chromatography (hexane/ethyl acetate, 1:5) afforded **1b** (16 mg, 91%) as a brown solid; mp 57–62 °C. R_f = 0.62 (hexane/ethyl acetate, 1:5). IR (CH_2Cl_2 , cast, cm^{-1}): 2934, 2193, 1750, 1587, 1433. 1H NMR (600 MHz, $CDCl_3$) δ : 5.51 (d, J = 3.5 Hz, 2H), 5.28 (t, J = 10.1 Hz, 2H), 5.09 (dd, J = 10.1 Hz, J = 3.5 Hz, 2H), 5.02 (s, 2H), 4.29 (dd, J = 12.3 Hz, J = 5.7 Hz, 2H), 4.13 (dd, J = 12.3 Hz, J = 2.4 Hz, 2H), 3.73 (d, J = 17.0 Hz, 4H), 3.71 (m, 2H), 3.43 (d, J = 17.0 Hz, 4H), 2.16 (s, 6H), 2.07 (s, 12 H), 2.04 (s, 12H), 1.97 (s, 6H). ^{13}C NMR (75 MHz, $CDCl_3$, APT) δ : 170.7, 170.1, 170.0, 169.7, 162.3, 99.7, 87.6, 80.9, 76.9, 76.4, 75.1, 72.1, 70.2, 69.6, 68.1, 65.8, 62.6, 31.8, 29.3, 23.4, 23.2, 20.80, 20.75, 20.66, 20.6. ESI-MS m/z (MeOH): 1029.3 ($[M + Na]^+$).

Compound 1c

Compound **4c** (68 mg, 0.24 mmol) was desilylated with K_2CO_3 in MeOH/THF (1:1) as described in general procedure A, and homocoupled in acetone (10 mL) in the presence of Hay catalyst (1 mL) and air for 0.5 h as described in general procedure C. Flash chromatography (hexane/ CH_2Cl_2 , 2:1) afforded **1c** (32 mg, 66%) as a yellow waxy solid. R_f = 0.61 (hexane/ CH_2Cl_2 , 2:1). UV-vis ($CHCl_3$) λ_{max} (ϵ): 282 (91 200), 296 (82 100), 322 (41 900), 349 (18 600), 374 (19 900), 405 (11 800). IR (μ scope, cm^{-1}): 3057, 2930, 2906, 2194, 2127, 1598, 1583, 1490, 1443. 1H NMR (300 MHz, $CDCl_3$) δ : 7.46–7.42 (m, 4H), 7.32–7.28 (m, 6H), 2.13 (s, 6H), 2.12 (s, 6H). ^{13}C NMR (75 MHz, $CDCl_3$, APT) δ : 161.5, 131.5, 128.5, 128.4, 122.9, 100.4, 92.9, 84.4, 76.4, 75.0, 67.9, 64.1, 23.4, 23.3. EI HR-MS calcd for $C_{32}H_{22}$ (M^+): 406.1722; found: 406.1728.

Compound 1d

Compound **4d** (88 mg, 0.27 mmol) was desilylated with K_2CO_3 in MeOH/THF (1:1) as described in general procedure A, and homocoupled in acetone (10 mL) in the presence of Hay catalyst (1 mL) and air for 0.5 h as described in general procedure C. Flash chromatography (hexane/ CH_2Cl_2 , 2:1) afforded **1d** (64 mg, 95%) as a yellow solid; mp > 115 °C (dec). R_f = 0.57 (hexane/ CH_2Cl_2 , 2:1). UV-vis ($CHCl_3$) λ_{max} (ϵ): 287 (66 700), 306 (90 400), 323 (83 700), 349 (50 200), 374 (39 800), 405 (15 900). IR (μ scope, cm^{-1}): 3104, 2932, 2847, 2198, 2128, 1594, 1520, 1491, 1432, 1343. 1H NMR (400 MHz, $CDCl_3$) δ : 8.17 (d, J = 8.8 Hz, 4H), 7.57 (d, J = 8.8 Hz, 4H), 2.149 (s, 6H), 2.146 (s, 6H). ^{13}C NMR (100 MHz, $CDCl_3$, APT) δ : 163.9, 147.1, 132.1, 129.7, 123.6, 99.9, 90.8, 89.5, 76.7, 74.2, 68.1, 63.9, 23.54, 23.47. EI HR-MS calcd for $C_{32}H_{20}N_2O_4$ (M^+): 496.1423; found: 496.1425. DSC: decomposition 172 °C (onset), 193 °C (peak).

Compound 1e

Compound **4e** (53 mg, 0.16 mmol) was desilylated with K_2CO_3 in MeOH/THF (1:1) as described in general procedure A, and homocoupled in acetone (10 mL) in the presence of Hay catalyst (1 mL) and air for 2 h as described in general procedure C. Flash chromatography (hexane/ CH_2Cl_2 , 2:1) afforded **1e** (11 mg, 27%) as a yellow waxy semisolid that

slowly decomposed over a period of hours to days. $R_f = 0.28$ (hexane/CH₂Cl₂, 2:1). UV-vis (CHCl₃) λ_{\max} (ϵ): 283 (72 300), 304 (63 000), 323 (52 600), 349 (28 500), 374 (27 000), 405 (14 700). IR (μ scope, cm⁻¹): 2927, 2200, 1608, 1567, 1528, 1479, 1438, 1336. ¹H NMR (400 MHz, CDCl₃) δ : 8.06 (dd, $J = 8.0, 1.2$ Hz, 2H), 7.66 (dd, $J = 8.0, 1.6$ Hz, 2H), 7.57 (td, $J = 8.0, 1.2$ Hz, 2H), 7.44 (td, $J = 8.0, 1.6$ Hz, 2H), 2.22 (s, 6H), 2.15 (s, 6H). ¹³C NMR (100 MHz, CDCl₃, APT) δ : 165.0, 149.0, 134.7, 132.9, 128.7, 124.7, 118.5, 100.1, 92.2, 88.0, 76.6, 74.3, 68.0, 64.0, 23.6, 23.5. EI HR-MS calcd for C₃₂H₂₀N₂O₄ (M⁺): 496.1423; found: 496.1419.

Compound 1f

Compound **4f** (77 mg, 0.24 mmol) was desilylated with K₂CO₃ in MeOH/THF (1:1) as described in general procedure A, and homocoupled in acetone (10 mL) in the presence of Hay catalyst (1 mL) and air for 0.5 h as described in general procedure C. Flash chromatography (hexane/CH₂Cl₂, 2:1) afforded **1f** (23 mg, 39%) as a yellow waxy semisolid that slowly decomposed over a period of hours to days. $R_f = 0.4$ (hexane/CH₂Cl₂, 2:1). UV-vis (CHCl₃) λ_{\max} (ϵ): 280 (98 100), 299 (87 500), 320 (54 200), 348 (20 100), 374 (21 400), 405 (13 300). IR (CH₂Cl₂, cast, cm⁻¹): 3087, 2197, 1536, 1346. ¹H NMR (300 MHz, CDCl₃) δ : 8.28–8.27 (m, 2H), 8.17–8.13 (m, 2H), 7.75–7.72 (m, 2H), 7.49 (t, $J = 8.1$ Hz, 2H), 2.152 (s, 6H), 2.146 (s, 6H). ¹³C NMR (75 MHz, CDCl₃, APT) δ : 163.4, 148.2, 137.1, 129.4, 126.3, 124.8, 123.1, 99.9, 90.2, 86.9, 74.3, 68.1, 64.0, 23.6, 23.5 (one coincident peak not observed). EI HR-MS calcd for C₃₂H₂₀N₂O₄ (M⁺): 496.1423; found: 496.1409.

Compound 1h

Compound **4h** (40 mg, 0.13 mmol) was desilylated with K₂CO₃ in MeOH/THF (1:1) as described in general procedure A, and homocoupled in acetone (10 mL) in the presence of Hay catalyst (1 mL) and air for 0.5 h as described in general procedure C. Flash chromatography (hexane/CH₂Cl₂, 2:1) afforded **1h** (22 mg, 74%) as a yellow waxy semisolid that slowly decomposed over a period of hours to days when stored neat. $R_f = 0.63$ (hexane/CH₂Cl₂, 2:1). UV-vis (CHCl₃) λ_{\max} (ϵ): 300 (104 400), 323 (69 600), 348 (17 600), 374 (17 700), 405 (9 700). IR (CH₂Cl₂, cast, cm⁻¹): 2228, 2194, 2126, 1959, 1603, 1450, 1432. ¹H NMR (300 MHz, CDCl₃) δ : 7.59 (d, $J = 8.4$ Hz, 4H), 7.51 (d, $J = 8.4$ Hz, 4H), 2.14 (s, 12H). ¹³C NMR (75 MHz, CDCl₃, APT) δ : 163.6, 132.1, 132.0, 127.8, 118.5, 111.8, 100.0, 91.1, 88.7, 76.7, 74.3, 68.1, 64.0, 23.6, 23.5. EI HR-MS calcd for C₃₄H₂₀N₂ (M⁺): 456.1627; found: 456.1629.

Compound 1i

Compound **4i** (93 mg, 0.26 mmol) was desilylated with K₂CO₃ in MeOH/THF (1:1) as described in general procedure A, and homocoupled in acetone/CH₂Cl₂ (1:1; 10 mL) in the presence of Hay catalyst (1 mL) and air for 0.5 h as described in general procedure C. Flash chromatography (hexane/CH₂Cl₂, 2:1) afforded **1i** (63 mg, 85%) as a yellow solid; mp > 110 °C (dec). $R_f = 0.21$ (hexane/CH₂Cl₂, 2:1). UV-vis (CHCl₃) λ_{\max} (ϵ): 288 (104 300), 322 (49 000), 349 (17 600), 375 (20 100), 406 (12 200). IR (CH₂Cl₂, cast, cm⁻¹): 2198, 1589, 1485, 1425. ¹H NMR (400 MHz, CDCl₃) δ : 7.43 (d, $J = 8.8$ Hz, 4H), 7.29 (d, $J = 8.8$ Hz, 4H), 2.11 (s, 12H). ¹³C NMR (100 MHz, CDCl₃, APT) δ : 162.0, 132.8, 131.6, 122.7,

121.8, 100.2, 91.7, 85.4, 76.4, 74.7, 67.9, 64.0, 23.4, 23.3. ESI HR-MS (MeOH/toluene, 1:1) calcd for C₃₂H₂₀⁷⁹Br₂ (M⁺): 561.9926; found: 561.9928. DSC: decomposition 123 °C (onset), 131 °C (peak).

Compound 1j

Compound **4j** (73 mg, 0.23 mmol) was desilylated with K₂CO₃ in MeOH/THF (1:1) as described in general procedure A, and homocoupled in acetone/CH₂Cl₂ (1:1; 10 mL) in the presence of Hay catalyst (1 mL) and air for 20 min as described in general procedure C. Flash chromatography (hexane/CH₂Cl₂, 2:1) afforded **1j** (43 mg, 76%) as a yellow solid; mp > 115 °C (dec). $R_f = 0.52$ (hexane/CH₂Cl₂, 2:1). UV-vis (CHCl₃) λ_{\max} (ϵ): 296 (94 600), 314 (92 000), 347 (46 900), 376 (24 000), 408 (12 800). IR (CHCl₃, cast, cm⁻¹): 2902, 2194, 2122, 1958, 1608, 1520, 1480, 1444. ¹H NMR (400 MHz, CDCl₃) δ : 7.31 (d, $J = 9.2$ Hz, 4H), 6.61 (d, $J = 9.2$ Hz, 4H), 2.96 (s, 12H), 2.10 (s, 6H), 2.09 (s, 6H). ¹³C NMR (100 MHz, CDCl₃, APT) δ : 159.5, 150.2, 132.6, 111.7, 109.6, 100.7, 94.1, 82.3, 75.9, 75.5, 67.8, 64.1, 40.1, 23.2, 23.1. ESI HR-MS (MeOH/toluene, 1:1) calcd for C₃₆H₃₂N₂ (M⁺): 492.2565; found: 492.2560. DSC: decomposition 157 °C (onset), 165 °C (peak).

Compound 1k

Compound **4k** (70 mg, 0.18 mmol) was desilylated with K₂CO₃ in MeOH/THF (1:1) as described in general procedure A, and homocoupled in acetone/CH₂Cl₂ (1:1; 10 mL) in the presence of Hay catalyst (1 mL) and air for 0.5 h as described in general procedure C. Flash chromatography (hexane/CH₂Cl₂, 2:1) afforded **1k** (42 mg, 75%) as an orange solid; mp > 120 °C (dec). $R_f = 0.4$ (hexane/CH₂Cl₂, 2:1). UV-vis (CHCl₃) λ_{\max} (ϵ): 298 (78 800), 349 (19 400), 376 (18 400), 407 (11 500). IR (μ scope, cm⁻¹): 3098, 2987, 2932, 2904, 2214, 2191, 1577, 1424. ¹H NMR (500 MHz, CDCl₃) δ : 4.42 (m, 4H), 4.20 (m, 14H), 2.08 (s, 6H), 2.07 (s, 6H). ¹³C NMR (125 MHz, CDCl₃, APT) δ : 159.9, 100.7, 91.9, 80.5, 76.0, 75.3, 71.4, 69.9, 68.9, 67.8, 64.8, 64.1, 23.4, 23.2. ESI HR-MS (MeOH/toluene, 3:1) calcd for C₄₀H₃₀Fe₂ (M⁺): 622.1046; found: 622.1043. DSC: decomposition 160 °C (onset), 187 °C (peak).

Compound 4a

Triflate **2** (108 mg, 0.333 mmol) was cross-coupled with 1-hexayne (30 mg, 0.36 mmol) in degassed THF (20 mL) in the presence of PdCl₂(PPh₃)₂ (12 mg, 0.017 mmol), diisopropylamine (2 mL), and CuI (6 mg, 0.03 mmol) for 3 h as described in general procedure B. Flash chromatography (hexane/CH₂Cl₂, 2:1) afforded **4a** (84 mg, 98%) as a colourless oil that slowly turned brown. $R_f = 0.75$ (hexane/CH₂Cl₂, 2:1). IR (CH₂Cl₂, cast, cm⁻¹): 2959, 2933, 2873, 2198, 2097. ¹H NMR (300 MHz, CDCl₃) δ : 2.32 (t, $J = 7.2$ Hz, 2H), 2.00 (s, 3H), 1.98 (s, 3H), 1.56–1.36 (m, 4H), 0.90 (t, $J = 6.9$ Hz, 3H), 0.18 (s, 9H). ¹³C NMR (125 MHz, CDCl₃, APT) δ : 157.0, 100.5, 93.3, 90.5, 88.1, 76.1, 75.4, 74.6, 30.8, 22.8, 22.7, 22.0, 19.1, 13.6, -0.4. EI-MS m/z (rel. intensity): 256 (M⁺, 100), 241 ([M - Me]⁺, 88). EI HR-MS calcd for C₁₇H₂₄Si (M⁺): 256.1647; found: 256.1642.

Compound 4b

Triflate **2** (32 mg, 0.099 mmol) was cross-coupled with 2-propynyl 2,3,4,6-*O*-acetyl-1-thio- β -D-mannopyranoside (40 mg, 0.099 mmol) in degassed THF (20 mL) in the pres-

ence of $\text{PdCl}_2(\text{PPh}_3)_2$ (3 mg, 0.004 mmol), diisopropylamine (2 mL), and CuI (1.5 mg, 0.0079 mmol) for 1 h as described in general procedure B. Flash chromatography (hexane / ethyl acetate, 3:1) afforded **4b** (37 mg, 65%) as a colourless solid vide infra; mp 54–57 °C. $R_f = 0.33$ (hexane / ethyl acetate, 3:1). IR (μscope , cm^{-1}): 2961, 2916, 2849, 2199, 2098, 1744, 1592, 1433. ^1H NMR (600 MHz, CDCl_3) δ : 5.51 (d, $J = 3.5$ Hz, 1H), 5.28 (t, $J = 10.0$ Hz, 1H), 5.09 (dd, $J = 10.0$ Hz, $J = 3.6$ Hz, 1H), 5.02 (s, 1H), 4.29 (dd, $J = 10.0$ Hz, $J = 0.6$ Hz, 1H), 4.13 (dd, $J = 10.0$ Hz, $J = 0.2$ Hz, 1H), 3.72 (d, $J = 16.7$ Hz, 1H), 3.70 (m, 1H), 3.42 (d, $J = 16.7$ Hz, 1H), 2.16 (s, 3H), 2.07 (s, 3H), 2.05 (s, 3H), 2.023 (s, 3H), 2.020 (s, 3H), 1.96 (s, 3H), 0.18 (s, 9H). ^{13}C NMR (75 MHz, CD_2Cl_2 , APT) δ : 170.8, 170.4, 170.2, 169.9, 160.4, 99.9, 91.6, 87.8, 87.5, 81.3, 79.8, 77.1, 76.3, 74.0, 72.3, 70.5, 66.0, 62.7, 30.1, 23.2, 23.0, 20.9, 20.7, 19.6, -0.4 (one coincident peak not observed). ESI HR-MS calcd for $\text{C}_{28}\text{H}_{36}\text{O}_9\text{NaSSi}$ ($[\text{M} + \text{Na}]^+$): 599.1742; found: 599.1740.

Compound 4c

Trimethylphenylethynylsilane (60 mg, 0.34 mmol) was desilylated with K_2CO_3 in THF/MeOH (1:1) as per general procedure A to give **3c**, which was cross-coupled with triflate **2** (109 mg, 0.336 mmol) in degassed THF (20 mL) in the presence of $\text{PdCl}_2(\text{PPh}_3)_2$ (12 mg, 0.017 mmol), diisopropylamine (2 mL), and CuI (6 mg, 0.03 mmol) for 50 min as described in general procedure B. Flash chromatography (hexane/ CH_2Cl_2 , 2:1) afforded **4c** (90 mg, 96%) as a colourless solid; mp 71–72 °C. $R_f = 0.63$ (hexane/ CH_2Cl_2 , 2:1). IR (CH_2Cl_2 , cast, cm^{-1}): 2960, 2904, 2199, 2094, 1594, 1489. ^1H NMR (400 MHz, CDCl_3) δ : 7.45–7.42 (m, 2H), 7.31–7.27 (m, 3H), 2.10 (s, 3H), 2.09 (s, 3H), 0.20 (s, 9H). ^{13}C NMR (100 MHz, CDCl_3 , APT) δ : 158.8, 131.4, 128.25, 128.19, 123.1, 100.5, 92.1, 90.9, 88.0, 85.0, 76.0, 73.8, 23.00, 23.06, -0.4. EI MS m/z (rel. intensity): 276.1 (M^+ , 100), 261.1 ($[\text{M} - \text{Me}]^+$, 88). EI HR-MS calcd for $\text{C}_{19}\text{H}_{20}\text{Si}$ (M^+): 276.1334; found: 276.1334.

Compound 4d

Trimethyl(4-nitrophenylethynyl)silane (75 mg, 0.34 mmol) was desilylated with K_2CO_3 in THF/MeOH (1:1) as described in general procedure A to give **3d**, which was cross-coupled with triflate **2** (109 mg, 0.336 mmol) in degassed THF (20 mL) in the presence of $\text{PdCl}_2(\text{PPh}_3)_2$ (12 mg, 0.017 mmol), diisopropylamine (2 mL), and CuI (6 mg, 0.03 mmol) for 50 min as described in general procedure B. Flash chromatography (hexane/ CH_2Cl_2 , 1:1) afforded **4d** (97 mg, 90%) as a yellow solid; mp 94–95 °C. $R_f = 0.40$ (hexane/ CH_2Cl_2 , 1:1). IR (CHCl_3 , cast, cm^{-1}): 2960, 2199, 2095, 1595, 1519, 1491, 1433, 1342. ^1H NMR (400 MHz, CDCl_3) δ : 8.15 (d, $J = 8.9$ Hz, 2H), 7.54 (d, $J = 8.9$ Hz, 2H), 2.11 (s, 6H), 0.19 (s, 9H). ^{13}C NMR (100 MHz, CDCl_3 , APT) δ : 161.2, 146.9, 132.0, 129.9, 123.5, 100.1, 91.5, 90.3, 90.2, 87.6, 76.6, 72.8, 23.22, 23.19, -0.5. EI MS m/z (rel. intensity): 321.1 (M^+ , 100), 306.1 ($[\text{M} - \text{Me}]^+$, 58). EI HR-MS calcd for $\text{C}_{19}\text{H}_{19}\text{NO}_2\text{Si}$ (M^+): 321.1185; found: 321.1180. Anal. calcd for $\text{C}_{19}\text{H}_{19}\text{NO}_2\text{Si}$: C 70.99, H 5.96; found: C 70.88, H 5.96.

Compound 4e

Trimethyl(2-nitrophenylethynyl)silane (75 mg, 0.34 mmol) was desilylated with K_2CO_3 in THF/MeOH (1:1) as described in general procedure A to give **3e**, which was cross-coupled with triflate **2** (109 mg, 0.336 mmol) in degassed THF (20 mL)

in the presence of $\text{PdCl}_2(\text{PPh}_3)_2$ (12 mg, 0.017 mmol), diisopropylamine (2 mL), and CuI (6 mg, 0.032 mmol) for 2 h as described in general procedure B. Flash chromatography (hexane/ CH_2Cl_2 , 1:1) afforded **4e** (95 mg, 87%) as a yellow solid; mp 93–94 °C. $R_f = 0.45$ (hexane/ CH_2Cl_2 , 1:1). IR (CH_2Cl_2 , cast, cm^{-1}): 2960, 2199, 2094, 1607, 1526, 1480, 1438, 1343. ^1H NMR (400 MHz, CDCl_3) δ : 8.02 (dd, $J = 8.3$, 1.2 Hz, 1H), 7.62 (dd, $J = 7.8$, 1.5 Hz, 1H), 7.54 (dt, $J = 7.5$, 1.3 Hz, 1H), 7.41 (dt, $J = 8.3$, 1.5 Hz, 1H), 2.17 (s, 3H), 2.11 (s, 3H), 0.19 (s, 9H). ^{13}C NMR (100 MHz, CDCl_3 , APT) δ : 162.4, 148.9, 134.6, 132.8, 128.5, 124.6, 118.6, 100.2, 93.0, 91.2, 87.9, 87.3, 76.3, 73.1, 23.3, 23.2, -0.4. EI MS m/z (rel. intensity): 321.1 (M^+ , 35), 73.0 (Me_3Si^+ , 100). EI HR-MS calcd for $\text{C}_{19}\text{H}_{19}\text{NO}_2\text{Si}$ (M^+): 321.1185; found: 321.1182. Anal. calcd for $\text{C}_{19}\text{H}_{19}\text{NO}_2\text{Si}$: C 70.99, H 5.96, N 4.36; found: C 71.10, H 5.95, N 4.29.

Compound 4f

Trimethyl(3-nitrophenylethynyl)silane (75 mg, 0.34 mmol) was desilylated with K_2CO_3 in THF/MeOH (1:1) as described in general procedure A to give **3f**, which was cross-coupled with triflate **2** (109 mg, 0.336 mol) in degassed THF (20 mL) in the presence of $\text{PdCl}_2(\text{PPh}_3)_2$ (12 mg, 0.017 mmol), diisopropylamine (2 mL), and CuI (6 mg, 0.032 mmol) for 10 min as described in general procedure B. Flash chromatography (hexane/ CH_2Cl_2 , 1:1) afforded **4f** (98 mg, 91%) as a yellow solid; mp 77–78 °C. $R_f = 0.49$ (hexane/ CH_2Cl_2 , 1:1). IR (CH_2Cl_2 , cast, cm^{-1}): 3084, 2960, 2904, 2200, 2095, 1572, 1532, 1477, 1433, 1351. ^1H NMR (400 MHz, CDCl_3) δ : 8.27–8.25 (m, 1H), 8.15–8.11 (m, 1H), 7.72 (dt, $J = 7.5$, 1.1 Hz, 1H), 7.48 (t, $J = 7.9$ Hz, 1H), 2.12 (s, 3H), 2.11 (s, 3H), 0.19 (s, 9H). ^{13}C NMR (75 MHz, CDCl_3 , APT) δ : 160.7, 148.2, 137.1, 129.4, 126.2, 125.0, 122.9, 100.1, 91.5, 89.6, 87.8, 87.7, 73.1, 23.3, 23.2, -0.4 (one signal coincident or not observed). EI MS m/z (rel. intensity): 321.1 (M^+ , 100), 306.1 ($[\text{M} - \text{Me}]^+$, 48). EI HR-MS calcd for $\text{C}_{19}\text{H}_{19}\text{NO}_2\text{Si}$ (M^+): 321.1185; found: 321.1176.

Compound 4g

Trimethyl(5-nitrothienyl-2-ylethynyl)silane (76 mg, 0.34 mmol) was desilylated with K_2CO_3 in THF/MeOH (1:1) as described in general procedure A to give **3g**, which was cross-coupled with triflate **2** (109 mg, 0.336 mmol) in degassed THF (20 mL) in the presence of $\text{PdCl}_2(\text{PPh}_3)_2$ (12 mg, 0.017 mmol), diisopropylamine (2 mL), and CuI (6 mg, 0.03 mmol) for 1 h as described in general procedure B. Flash chromatography (hexane/ CH_2Cl_2 , 2:1) afforded **4g** (40 mg, 36%) as a yellow solid; mp 68–69 °C. $R_f = 0.18$ (hexane/ CH_2Cl_2 , 1:1). IR (CH_2Cl_2 , cast, cm^{-1}): 3108, 2960, 2196, 2097, 1587, 1531, 1503, 1430, 1332. ^1H NMR (400 MHz, CDCl_3) δ : 7.77 (d, $J = 4.4$ Hz, 1H), 7.06 (d, $J = 4.4$ Hz, 1H), 2.11 (s, 3H), 2.09 (s, 3H), 0.20 (s, 9H). ^{13}C NMR (100 MHz, CDCl_3 , APT) δ : 162.4, 150.8, 130.8, 130.6, 128.5, 99.8, 93.8, 91.9, 87.5, 83.6, 77.0, 72.1, 23.4, 23.3, -0.5. EI HR-MS calcd for $\text{C}_{17}\text{H}_{17}\text{NO}_2\text{SSi}$ (M^+): 327.0749; found: 327.0749.

Compound 4h

4-Trimethylsilylethynylbenzonitrile (43 mg, 0.22 mmol) was desilylated with K_2CO_3 in THF/MeOH (1:1) as described in general procedure A to give **3h**, which was cross-coupled with triflate **2** (70 mg, 0.22 mmol) in degassed THF (20 mL) in the presence of $\text{PdCl}_2(\text{PPh}_3)_2$ (6 mg, 0.009 mmol), diiso-

propylamine (2 mL), and CuI (3 mg, 0.02 mmol) for 1.5 h as described in general procedure B. Flash chromatography (hexane/CH₂Cl₂, 1:1) afforded **4h** (52 mg, 80%) as a yellow solid; mp 60–62 °C. *R_f* = 0.48 (hexane/CH₂Cl₂, 1:1). IR (CH₂Cl₂, cast, cm⁻¹): 2960, 2904, 2229, 2199, 2095, 1604, 1499, 1433. ¹H NMR (400 MHz, CDCl₃) δ: 7.59 (d, *J* = 8.6 Hz, 2H), 7.50 (d, *J* = 8.6 Hz, 2H), 2.11 (s, 6H), 0.20 (s, 9H). ¹³C NMR (75 MHz, CDCl₃, APT) δ: 160.9, 132.0, 131.9, 128.1, 118.5, 111.6, 100.2, 91.5, 90.4, 89.5, 87.7, 73.0, 23.3, -0.4 (two coincident peaks not observed). EI MS *m/z* (rel. intensity): 301.1 (M⁺, 93), 286.1 ([M - Me]⁺, 100). EI HR-MS calcd for C₂₀H₁₉NSi (M⁺): 301.1287; found: 301.1292.

Compound 4i

(4-Bromophenylethynyl)trimethylsilane (101 mg, 0.399 mmol) was desilylated with K₂CO₃ in THF/MeOH (1:1) as described in general procedure A to give **3i**, which was cross-coupled with triflate **2** (130 mg, 0.401 mmol) in degassed THF (20 mL) in the presence of PdCl₂(PPh₃)₂ (14 mg, 0.020 mmol), diisopropylamine (2 mL), and CuI (7 mg, 0.04 mmol) for 2 h as described in general procedure B. Flash chromatography (hexane/CH₂Cl₂, 1:1) afforded **4i** (112 mg, 79%) as a colourless waxy solid. *R_f* = 0.80 (hexane/CH₂Cl₂, 1:1). IR (CHCl₃, cast, cm⁻¹): 2959, 2198, 2094, 1484, 1421. ¹H NMR (400 MHz, CDCl₃) δ: 7.42 (d, *J* = 8.4 Hz, 2H), 7.28 (d, *J* = 8.4 Hz, 2H), 2.08 (s, 6H), 0.20 (s, 9H). ¹³C NMR (75 MHz, CDCl₃, APT) δ: 159.3, 132.8, 131.5, 122.5, 122.0, 100.4, 91.1, 91.0, 87.9, 86.2, 76.2, 73.5, 23.1, 23.0, -0.4. EI HR-MS calcd for C₁₉H₁₉⁸¹BrSi (M⁺): 356.0419; found: 356.0419.

Compound 4j

N,N-Dimethyl(4-trimethylsilylethynylphenyl)amine (109 mg, 0.501 mmol) was desilylated with K₂CO₃ in THF/MeOH (1:1) as described in general procedure A to give **3j**, which was cross-coupled with triflate **2** (162 mg, 0.501 mmol) in degassed THF (20 mL) in the presence of PdCl₂(PPh₃)₂ (18 mg, 0.026 mmol), diisopropylamine (2 mL), and CuI (9 mg, 0.05 mmol) for 1.5 h as described in general procedure B. Flash chromatography (hexane/CH₂Cl₂, 2:1) afforded **4j** (133 mg, 83%) as a yellow solid; mp 82–83 °C. *R_f* = 0.50 (hexane/CH₂Cl₂, 2:1). IR (CHCl₃, cast, cm⁻¹): 2959, 2902, 2200, 2094, 1609, 1521, 1481, 1445. ¹H NMR (400 MHz, CDCl₃) δ: 7.30 (d, *J* = 8.8 Hz, 2H), 6.60 (d, *J* = 8.8 Hz, 2H), 2.96 (s, 6H), 2.09 (s, 3H), 2.07 (s, 3H), 0.22 (s, 9H). ¹³C NMR (100 MHz, CDCl₃, APT) δ: 156.9, 150.0, 132.5, 111.7, 109.8, 100.9, 93.3, 90.5, 88.2, 82.9, 75.6, 74.4, 40.1, 22.9, 22.8, -0.4. EI HR-MS calcd for C₂₁H₂₅NSi (M⁺): 319.1756; found: 319.1750. Anal. calcd for C₂₁H₂₅NSi: C 78.94, H 7.89, N 4.38; found: C 78.70, H 8.04, N 4.47.

Compound 4k

Ethynylferrocene **3k** (76 mg, 0.36 mmol) was cross-coupled with triflate **2** (117 mg, 0.362 mmol) in degassed THF (20 mL) in the presence of PdCl₂(PPh₃)₂ (13 mg, 0.018 mmol), diisopropylamine (2 mL), and CuI (7 mg, 0.04 mmol) for 2 h as described in general procedure B. Flash chromatography (hexane/CH₂Cl₂, 2:1) afforded **4k** (78 mg, 56%) as a yellow solid; mp 84–85 °C. *R_f* = 0.82 (hexane/CH₂Cl₂, 2:1). IR (μscope, cm⁻¹): 3099, 2964, 2908, 2214, 2191, 2091, 1593, 1426, 1410. ¹H NMR (600 MHz, CDCl₃) δ: 4.42 (t, *J* = 1.8 Hz, 2H), 4.21 (s, 5H), 4.19 (t, *J* = 1.8 Hz, 2H), 2.06 (s, 3H), 2.05 (s, 3H), 0.19 (s, 9H). ¹³C NMR (75 MHz, CDCl₃,

APT) δ: 157.6, 100.9, 91.1, 90.7, 88.1, 81.2, 74.2, 71.4, 70.0, 68.8, 65.1, 23.1, 22.9, -0.3 (one coincident peak not observed). EI HR-MS calcd for C₂₃H₂₄FeSi (M⁺): 384.0997; found: 384.1001.

Compound 6a

Compound **10a** (62.5 mg, 0.164 mmol) was desilylated with K₂CO₃ in MeOH/THF (1:1) as described in general procedure A, and the resulting product was subjected to a homocoupling reaction in CH₂Cl₂ (60 mL) in the presence of Hay catalyst (1 mL) and air as described in general procedure C. Flash chromatography (hexanes/CH₂Cl₂, 7:1) gave **6a** (38.0 mg, 75%) as a yellow crystalline solid; mp 185 °C (dec). *R_f* = 0.46 (hexanes/CH₂Cl₂, 7:1). UV-vis (THF) λ_{max} (ε): 299 (66 600), 314 (78 600), 330 (64 700), 359 (27 600), 386 (30 600), 419 (19 500). IR (CHCl₃, cast, cm⁻¹): 3010, 2192, 1524, 1488. ¹H NMR (500 MHz, CDCl₃) δ: 7.36 (s). ¹³C NMR (100 MHz, CDCl₃) δ: 136.6, 129.5, 129.1, 128.7, 128.5, 105.3, 81.9, 76.5, 70.9, 64.9. EI MS *m/z* (rel. intensity): 617.7 (M⁺, 80), 298.1 ([M - 4Br]⁺, 100). HR-MS calcd for C₂₄H₁₀⁷⁹Br₂⁸¹Br₂ (M⁺): 617.7475; found: 617.7488. Anal. calcd for C₂₄H₁₀Br₄: C 46.66, H 1.63; found: C 46.35, H 1.46. DSC: decomposition 191 °C (onset), 192 °C (peak).

Compound 6b

Compound **10b** (582 mg, 1.42 mmol) was desilylated with K₂CO₃ in MeOH/THF (1:1) as described in general procedure A, and the resulting product was subjected to a homocoupling reaction in CH₂Cl₂ (60 mL) in the presence of Hay catalyst (1 mL) and air as described in general procedure C. Flash chromatography (hexanes/CH₂Cl₂, 3:1) gave **6b** (223 mg, 46%) as a yellow-green solid; mp 168–170 °C. *R_f* = 0.41 (hexanes/CH₂Cl₂, 3:1). UV-vis (THF) λ_{max} (ε): 296 (80 200, sh), 308 (93 100), 331 (59 200, sh), 360 (26 900), 388 (27 800), 420 (18 300). IR (CHCl₃, cast, cm⁻¹): 2924, 2190, 1605, 1505, 1252. ¹H NMR (300 MHz, CDCl₃) δ: 7.32 (d, *J* = 9.0 Hz, 4H), 6.88 (d, *J* = 9.0 Hz, 4H), 3.81 (s, 6H). ¹³C NMR (100 MHz, CDCl₃, APT) δ: 156.0, 123.0, 129.1, 128.8, 114.0, 104.2, 81.7, 70.9, 65.0, 55.3 (one signal coincident or not observed). EI HR-MS calcd for C₂₆H₁₄⁷⁹Br₂⁸¹Br₂O₂ (M⁺): 677.7686; found: 677.7697. Anal. calcd for C₂₆H₁₄Br₄O₂: C 46.06, H 2.08; found: C 45.87, H 1.93. DSC: mp 176 °C; decomposition 176 °C (onset), 179 °C (peak).

Compound 6c

Compound **10c** (401 mg, 0.914 mmol) was desilylated with K₂CO₃ in MeOH/THF (1:1) as described in general procedure A, and the resulting product was subjected to a homocoupling reaction in CH₂Cl₂ (60 mL) in the presence of Hay catalyst (1 mL) and air as described in general procedure C. Flash chromatography (hexanes/CH₂Cl₂, 7:1) gave **6c** (265 mg, 80%) as a yellow crystalline solid; mp 168–179 °C (dec). *R_f* = 0.52 (hexanes/CH₂Cl₂, 7:1). UV-vis (THF) λ_{max} (ε): 299 (72 100), 309 (70 500), 331 (55 100), 359 (25 200), 387 (27 600), 419 (17 500). IR (CHCl₃, cast, cm⁻¹): 2963, 2182, 1531. ¹H NMR (300 MHz, CDCl₃) δ: 7.38 (d, *J* = 8.7 Hz, 4H), 8.7 (d, *J* = 8.7 Hz, 4H), 1.30 (s, 18H). ¹³C NMR (100 MHz, CDCl₃) δ: 152.3, 133.5, 129.4, 128.2, 125.6, 104.6, 81.8, 77.3, 70.9, 65.0, 34.9, 31.3. EI HR-MS calcd for C₃₂H₂₆⁷⁹Br₂⁸¹Br₂ (M⁺): 729.8727; found: 729.8750. DSC: decomposition initial onset ~200 °C; 229 °C (onset), 233 °C (peak).

Compound 6d

Compound **10d** (1.10 g, 2.58 mmol) was desilylated with K_2CO_3 in MeOH/THF (1:1) as described in general procedure A, and the resulting product was subjected to a homocoupling reaction in CH_2Cl_2 (60 mL) in the presence of Hay catalyst (1 mL) and air as described in general procedure C. Flash chromatography (hexanes/ CH_2Cl_2 , 1:1) gave **6d** (469 mg, 51%) as a yellow crystalline solid; mp > 190 °C (dec). R_f = 0.4 (hexanes/ CH_2Cl_2 , 1:1). UV-vis (THF) λ_{max} (ϵ): 296 (80 200), 312 (106 200), 331 (80 000), 359 (29 200), 387 (31 700), 419 (19 900). IR ($CHCl_3$, cast, cm^{-1}): 3104, 2188, 2114, 1517, 1346. 1H NMR (400 MHz, $CDCl_3$) δ : 8.24 (d, J = 9.2 Hz, 4H), 7.57 (d, J = 9.2 Hz, 4H). ^{13}C NMR (100 MHz, $CDCl_3$) δ : 147.8, 142.5, 129.6, 127.4, 123.8, 107.5, 82.6, 75.4, 71.2, 64.8. EI MS m/z (rel. intensity): 707.7 (M^+ , 23), 388.0 ($[M - 4Br]^+$, 6). HR-MS calcd for $C_{24}H_8^{79}Br_2^{81}Br_2N_2O_4$: 707.7177 (M^+); found: 707.7217. Anal. calcd for $C_{24}H_8Br_4N_2O_4$: C 40.72, H 1.14, N 3.96; found: C 40.94, H 1.10, N 3.80. DSC: decomposition 189 °C (onset), 191 °C (peak).

Compound 10d

Under an inert atmosphere of nitrogen, 4-nitrobenzoyl chloride (2.45 g, 13.2 mmol) and bis(trimethylsilyl)butadiyne (**8**; 2.30 g, 11.8 mmol) were dissolved in CH_2Cl_2 (100 mL) and the temperature of the solution lowered to -20 °C. $AlCl_3$ (2.4 g, 18.0 mmol) was added slowly over ~1 min, the cooling bath removed, and the reaction mixture allowed to warm to rt over ~3 h. The reaction was carefully quenched by the addition of the reaction mixture to 10% HCl (50 mL) in ice (50 mL). (Caution: This step is exothermic and can cause the CH_2Cl_2 to boil!) Et_2O (70 mL) was added, the organic layer separated, washed with saturated aq $NaHCO_3$ (2×20 mL) and brine (2×20 mL), dried over $MgSO_4$, and the solvent removed in vacuo. The resulting product **9d** was carried on to the next step without further purification.

CBr_4 (3.15 g, 9.50 mmol) and PPh_3 (5.00 g, 19.1 mmol) were added to CH_2Cl_2 (100 mL) at 0 °C and the solution stirred for ~5 min at rt until the mixture turned orange. The ketone **9d**, dissolved in CH_2Cl_2 (~5 mL), was added in one portion. The reaction was allowed to warm to rt and monitored by TLC analysis until the ketone was no longer observed (~1 h). When the reaction was judged complete, the solvent was reduced to ~5 mL, hexanes (50 mL) were added, the inhomogeneous mixture filtered through a plug of Celite layered on top of silica gel, and the resulting filtrate was concentrated in vacuo. This process can be repeated a second time if necessary to remove phosphine/phosphonium byproducts. Column chromatography (silica gel, hexanes/ CH_2Cl_2 , 1:1) gave **10d** (2.54 g, 51%) as a cream-coloured powder; mp 80–83 °C. R_f = 0.60 (hexanes/ CH_2Cl_2 , 1:1). IR ($CHCl_3$, cast film, cm^{-1}): 2960, 2096, 1595, 1523. 1H NMR (300 MHz, $CDCl_3$) δ : 8.22 (d, J = 8.7 Hz, 2H), 7.58 (d, J = 8.7 Hz, 2H), 0.19 (s, 9H). ^{13}C NMR (125 MHz, $CDCl_3$, APT) δ : 147.7, 143.4, 129.7, 128.1, 123.8, 104.8, 96.7, 86.8, 83.2, 73.8, -0.6. EI MS m/z (rel. intensity): 426.9 (M^+ , 28), 411.9 ($[M - CH_3]^+$, 100). HR-MS calcd for $C_{15}H_{13}NO_2Si^{79}Br^{81}Br$ (M^+): 426.9062; found: 426.9064. Anal. calcd for $C_{15}H_{13}NO_2SiBr_2$: C 42.18, H 3.07, N 3.28; found: C 42.30, H 2.81, N 3.16.

Compound 11

$^{13}CBr_4$ (287 mg, 0.865 mmol), CBr_4 (431 mg, 1.30 mmol), and PPh_3 (1.14 g, 4.33 mmol) were added to CH_2Cl_2 (15 mL) at 0 °C and the solution stirred for ~5 min at rt until the mixture turned bright orange. Triisopropylsilylpropargylaldehyde (501 mg, 2.38 mmol) dissolved in CH_2Cl_2 (~2 mL) was added in one portion. The reaction was allowed to warm to rt and monitored by TLC analysis until the ketone was no longer observed (~1 h). When the reaction was judged complete, the solvent was reduced to ~5 mL, hexanes (25 mL) were added, the inhomogeneous mixture filtered through a plug of Celite layered on top of silica gel, and the resulting filtrate concentrated in vacuo. This process can be repeated a second time if necessary to remove phosphine/phosphonium byproducts. Column chromatography gave **11** (638 mg, 73%) with ~34% labelling. Spectral data are consistent with those previously reported, see ref. 35. 1H NMR (500 MHz, $CDCl_3$) δ : 6.59 (d, J = 1.5 Hz, 1H), 1.08 (s, 21H). ^{13}C NMR (125 MHz, $CDCl_3$) δ : 120.0 (d, 1J = 360 Hz), 102.9 (C^* , s and d, 1J = 360 Hz), 102.5 (s), 100.8 (d, 3J = 25 Hz), 18.6, 11.1.

Compound 12

To a solution of compound **11** (638 mg, 1.74 mmol) in Et_2O (2 mL) at -78 °C was added via cannula a solution of LDA (formed from BuLi (2.5 mol/L in hexanes, 2.1 mL, 5.3 mmol) and diisopropylamine (0.73 mL, 0.53 mg, 5.23 mmol) in Et_2O (17 mL)) at -78 °C, and the resulting solution was stirred for 2 h at -78 °C. To this mixture was added dropwise Me_3SiCl (0.33 mL, 0.28 mg, 2.61 mmol). The reaction was allowed to warm to rt and stirred overnight. Et_2O (10 mL) and saturated aq NH_4Cl (10 mL) were added. The organic phase was separated, washed with brine (2×10 mL), and dried over $MgSO_4$. Solvent removal and purification by column chromatography (silica gel, hexanes) afforded **12** (325 mg, 67%) as a colourless oil. R_f = 0.67 (hexanes), which was carried on to the next step without further purification.

Compound 14

Under an inert atmosphere of nitrogen, 4-nitrobenzoyl chloride (239 mg, 1.29 mmol) and compound **12** (321 mg, 1.15 mmol) were dissolved in CH_2Cl_2 (12 mL) and the temperature of the solution lowered to -20 °C. $AlCl_3$ (230 mg, 1.72 mmol) was added slowly over ~1 min, the cooling bath removed, and the reaction mixture allowed to warm to rt over ~3 h. The reaction was carefully quenched by the addition of the reaction mixture to 10% HCl (25 mL) in ice (25 mL). (Caution: This step is exothermic and can cause the CH_2Cl_2 to boil!) Et_2O (50 mL) was added, the organic layer separated, washed with saturated aq $NaHCO_3$ (2×20 mL) and brine (2×20 mL), dried over $MgSO_4$, and the solvent removed in vacuo to give ketone **13** as a colourless oil. The ketone **13** was carried on to the next step without further purification.

CBr_4 (764 mg, 2.30 mmol) and PPh_3 (1.21 g, 4.61 mmol) were added to CH_2Cl_2 (12 mL) at 0 °C and the solution stirred for ~5 min at rt until the mixture turned bright orange. Ketone **13**, dissolved in CH_2Cl_2 (~2 mL), was added in one portion. The reaction was allowed to warm to rt and monitored by TLC analysis until the ketone was no longer observed (~1 h). When the reaction was judged complete, the solvent was reduced to ~5 mL, hexanes (50 mL) were added, and the inhomogeneous mixture filtered through a plug of Celite layered on top of silica gel. The resulting filtrate was concentrated in vacuo to give compound **14** (206 mg, 35%) as a colourless oil.

^{13}C NMR (125 MHz, CDCl_3) δ : 147.7, 143.5, 129.7, 128.3 (d, $J = 98$ Hz), 123.8, 104.5, 94.3, 88.5 (d, $J = 18$ Hz), 83.6 (d, $J = 202$ Hz), 72.7 (C*, m), 18.5, 11.2.

Compounds 6d/6d*/6d**

To compound **14** (206 mg, 0.403 mmol) in THF (6 mL) was added TBAF (1.0 mol/L in THF, 0.52 mL, 0.52 mmol). The solution was stirred at rt until TLC analysis showed complete conversion to the terminal alkyne. Et_2O and saturated aq NH_4Cl were added, the organic phase was separated, washed with saturated aq NH_4Cl (2×10 mL) and brine (10 mL), and then dried over MgSO_4 . The solution was concentrated to 1–2 mL via rotary evaporation and diluted with CH_2Cl_2 (6 mL). Hay catalyst (1 mL) was added and the reaction continued as described in general procedure C to give a mixture of isotopomers **6d/6d*/6d**** (59.7 mg, 42%). Spectral data were consistent with those of **6d**. ^{13}C NMR (125 MHz, CDCl_3) δ : 147.9, 142.7, 129.7, 127.6 (d, $J = 98$ Hz), 124.0, 107.6, 82.7 (d, $J = 187$ Hz), 75.6 (C*, m), 71.4 (d, $J = 32$ Hz), 64.9.

Supplementary data

Supplementary data are available with the article through the journal Web site at <http://nrcresearchpress.com/doi/suppl/10.1139/v2012-075>. CCDC HOZSAQ and 862755–862758 contain the X-ray data in CIF format for this manuscript. These data can be obtained, free of charge, via <http://www.ccdc.cam.ac.uk/products/csd/request> (or from the Cambridge Crystallographic Data Centre, 12 Union Road, Cambridge CB2 1EZ, UK; fax: 44 1223 336033; or e-mail: deposit@ccdc.cam.ac.uk).

Acknowledgments

We are grateful for financial support for this work as provided by the University of Alberta, the Alberta Ingenuity Fund, the Natural Sciences and Engineering Research Council of Canada (NSERC), and Petro Canada (Young Innovator Award to R.R.T.). R.E.W. is a Canada Research Chair in Physical Chemistry at the University of Alberta.

References

- Hoheisel, T. N.; Schrettl, S.; Szilluweit, R.; Frauenrath, H. *Angew. Chem. Int. Ed.* **2010**, *49* (37), 6496. doi:10.1002/anie.200907180.
- Yoon, B.; Lee, S.; Kim, J. M. *Chem. Soc. Rev.* **2009**, *38* (7), 1958. doi:10.1039/b819539k.
- Sun, X. M.; Chen, T.; Huang, S. Q.; Li, L.; Peng, H. S. *Chem. Soc. Rev.* **2010**, *39* (11), 4244. doi:10.1039/c001151g.
- Reppy, M. A.; Pindzola, B. A. *Chem. Commun. (Camb.)* **2007**, (42): 4317. doi:10.1039/b703691d.
- Carpick, R. W.; Sasaki, D. Y.; Marcus, M. S.; Eriksson, M. A.; Burns, A. R. *J. Phys. Condens. Matter* **2004**, *16* (23), R679. doi:10.1088/0953-8984/16/23/R01.
- Materny, A.; Chen, T.; Vierheilig, A.; Kiefer, W. *J. Raman Spectrosc.* **2001**, *32* (6–7), 425. doi:10.1002/jrs.716.
- Zhou, W. D.; Li, Y. L.; Zhu, D. B. *Chem. Asian J.* **2007**, *2* (2), 222. doi:10.1002/asia.200600218.
- Ahn, D. J.; Kim, J. M. *Acc. Chem. Res.* **2008**, *41* (7), 805. doi:10.1021/ar7002489.
- Bässler, H. *Adv. Polym. Sci.* **1984**, *63*, 1. doi:10.1007/BFb0017650.

- Baughman, R. H. *J. Polym. Sci., Polym. Phys. Ed.* **1974**, *12* (8), 1511. doi:10.1002/pol.1974.180120801.
- Bloor, D.; Chance, R. R., Eds. *Polydiacetylenes*; Martinus Nijhoff: Dordrecht, 1985.
- Wegner, G. *Z. Naturforsch.* **1969**, *24b*, 824.
- Szafert, S.; Gladysz, J. A. *Chem. Rev.* **2006**, *106* (11), PR1. doi:10.1021/cr068016g.
- Enkelmann, V. *Adv. Polym. Sci.* **1984**, *63*, 91. doi:10.1007/BFb0017652.
- Baughman, R. H.; Yee, K. C. *J. Polym. Sci.: Macromol. Rev.* **1978**, *13* (1), 219. doi:10.1002/pol.1978.230130104.
- Paley, M. S.; Frazier, D. O.; Abeledyem, H.; McManus, S. P.; Zutaut, S. E. *J. Am. Chem. Soc.* **1992**, *114* (9), 3247. doi:10.1021/ja00035a013.
- For reviews see: (a) Lauher, J. W.; Fowler, F. W.; Goroff, N. S. *Acc. Chem. Res.* **2008**, *41* (9), 1215. doi:10.1021/ar8001427; (b) Sarkar, A.; Okada, S.; Matsuzawa, H.; Matsuda, H.; Nakanishi, H. *J. Mater. Chem.* **2000**, *10* (4), 819. doi:10.1039/a907438d; (c) Fowler, F. W.; Lauher, J. W. *J. Phys. Org. Chem.* **2000**, *13* (12), 850. doi:10.1002/1099-1395(200012)13:12<850::AID-POC316>3.0.CO;2-L.
- For theoretical predictions see Yang, S.; Kertesz, M. *Macromolecules* **2007**, *40* (18), 6740. doi:10.1021/ma0708040.
- For examples see: (a) Xu, R.; Schweizer, W. B.; Frauenrath, H. *Chemistry* **2009**, *15* (36), 9105. doi:10.1002/chem.200900985; (b) Mizukoshi, K.; Okada, S.; Kimura, T.; Shimada, S.; Matsuda, H. *Bull. Chem. Soc. Jpn.* **2008**, *81* (8), 1028. doi:10.1246/bcsj.81.1028; (c) Xiao, J.; Yang, M.; Lauher, J. W.; Fowler, F. W. *Angew. Chem. Int. Ed.* **2000**, *39* (12), 2132. doi:10.1002/1521-3773(20000616)39:12<2132::AID-ANIE2132>3.0.CO;2-8; (d) Hlavatý, J.; Kavan, L.; Kasahara, N.; Oya, A. *Chem. Commun. (Camb.)* **2000**, (9): 737. doi:10.1039/b000895h; (e) Enkelmann, V. *Chem. Mater.* **1994**, *6* (8), 1337. doi:10.1021/cm00044a035; (f) Okada, S.; Hayamizu, K.; Matsuda, H.; Masaki, A.; Nakanishi, H. *Bull. Chem. Soc. Jpn.* **1991**, *64* (3), 857. doi:10.1246/bcsj.64.857; (g) Kiji, J.; Kaiser, J.; Wegner, G.; Schulz, R. C. *Polymer (Guildf.)* **1973**, *14* (9), 433. doi:10.1016/0032-3861(73)90009-8.
- (a) Rubin, Y.; Lin, S. S.; Knobler, C. B.; Anthony, J.; Boldi, A. M.; Diederich, F. *J. Am. Chem. Soc.* **1991**, *113* (18), 6943. doi:10.1021/ja00018a035; (b) Okada, S.; Nakanishi, H.; Matsuzawa, H.; Katagi, H.; Oshikiri, T.; Kasai, H.; Sarkar, A.; Oikawa, H.; Rangel-Rojo, R.; Fukuda, T.; Matsuda, H. *SPIE* **1999**, *3796*, 76. doi:10.1117/12.368302.
- For examples see: (a) Inayama, S.; Tatewaki, Y.; Okada, S. *Polym. J.* **2010**, *42* (3), 201. doi:10.1038/pj.2009.326; (b) Okada, S.; Hayamizu, K.; Matsuda, H.; Masaki, A.; Minami, N.; Nakanishi, H. *Macromolecules* **1994**, *27* (22), 6259. doi:10.1021/ma00100a005.
- For examples see: (a) Chen, G. A.; Mahmud, I.; Dawe, L. N.; Daniels, L. M.; Zhao, Y. *J. Org. Chem.* **2011**, *76* (8), 2701. doi:10.1021/jo2000447; (b) Ding, L. H.; Olesik, S. V. *Chem. Mater.* **2005**, *17* (9), 2353. doi:10.1021/cm048781g; (c) Li, T. S.; Okada, S.; Nakanishi, H. *Polym. Bull.* **2003**, *51* (2), 103. doi:10.1007/s00289-003-0199-z; (d) Sarkar, A.; Okada, S.; Komatsu, K.; Nakanishi, H.; Matsuda, H. *Macromolecules* **1998**, *31* (17), 5624. doi:10.1021/ma9803077; (e) Hayamizu, K.; Okada, S.; Doi, T.; Kawanami, H.; Kikuchi, N.; Matsuda, H.; Nakanishi, H. *Bull. Chem. Soc. Jpn.* **1995**, *68* (3), 791. doi:10.1246/bcsj.68.791.

- (23) (a) Jahnke, E.; Tykwinski, R. R. *Chem. Commun. (Camb.)* **2010**, 46 (19), 3235. doi:10.1039/c003170d; (b) Chalifoux, W. A.; Tykwinski, R. R. *C. R. Chim.* **2009**, 12 (3-4), 341. doi:10.1016/j.crci.2008.10.004.
- (24) For the stepwise formation of polytriacylenes see Martin, R. E.; Gunter, P.; Bosshard, C.; Gubler, U.; Gramlich, V.; Gross, M.; Boudon, C.; Gisselbrecht, J. P.; Diederich, F. *Chem. Eur. J.* **1997**, 3 (9), 1505 and references therein. doi:10.1002/chem.19970030919.
- (25) For reviews of cross-conjugated systems see: (a) Gholami, M.; Tykwinski, R. R. *Chem. Rev.* **2006**, 106 (12), 4997. doi:10.1021/cr0505573; (b) Nielsen, M. B.; Diederich, F. *Chem. Rev.* **2005**, 105 (5), 1837. doi:10.1021/cr9903353; (c) Hopf, H. *Angew. Chem. Int. Ed. Engl.* **1984**, 23 (12), 948. doi:10.1002/anie.198409481.
- (26) Tykwinski, R. R.; Zhao, Y. *Synlett* **2002**, (12): 1939. doi:10.1055/s-2002-35578.
- (27) The synthesis of **11** and **41** has been reported; see: (a) Zhao, Y.; McDonald, R.; Tykwinski, R. R. *J. Org. Chem.* **2002**, 67 (9), 2805. doi:10.1021/jo015995y; (b) Zhao, Y.; McDonald, R.; Tykwinski, R. R. *Chem. Commun. (Camb.)* **2000**, (1): 77. doi:10.1039/a906900c.
- (28) (a) Chinchilla, R.; Najera, C. *Chem. Rev.* **2007**, 107 (3), 874. doi:10.1021/cr050992x; (b) Tykwinski, R. R. *Angew. Chem. Int. Ed.* **2003**, 42 (14), 1566. doi:10.1002/anie.200201617; (c) Sonogashira, K.; Tohda, Y.; Hagihara, N. *Tetrahedron Lett.* **1975**, 16 (50), 4467. doi:10.1016/S0040-4039(00)91094-3.
- (29) Stang, P. J.; Ladika, M. *Synthesis* **1981**, (1), 29. doi:10.1055/s-1981-29318.
- (30) Hay, A. S. *J. Org. Chem.* **1962**, 27 (9), 3320. doi:10.1021/jo01056a511.
- (31) Luu, T.; Elliott, E.; Slepko, A. D.; Eisler, S.; McDonald, R.; Hegmann, F. A.; Tykwinski, R. R. *Org. Lett.* **2005**, 7 (1), 51. doi:10.1021/ol047931q.
- (32) Walton, D. R. M.; Waugh, F. *J. Organomet. Chem.* **1972**, 37 (1), 45. doi:10.1016/S0022-328X(00)89260-8.
- (33) Desai, N. B.; McKelvie, N.; Ramirez, F. *J. Am. Chem. Soc.* **1962**, 84 (9), 1745. doi:10.1021/ja00868a057.
- (34) For representative examples see refs. 19a, 19b, 19f, 21a, 21b, 22d, and 22e.
- (35) Eisler, S.; Slepko, A. D.; Elliott, E.; Luu, T.; McDonald, R.; Hegmann, F. A.; Tykwinski, R. R. *J. Am. Chem. Soc.* **2005**, 127 (8), 2666. doi:10.1021/ja044526l.
- (36) Luu, T.; Medos, B. J.; Graham, E. R.; Vallee, D. M.; McDonald, R.; Ferguson, M. J.; Tykwinski, R. R. *J. Org. Chem.* **2010**, 75 (24), 8498. doi:10.1021/jo101870y.
- (37) Eisler, S.; McDonald, R.; Loppnow, G. R.; Tykwinski, R. R. *J. Am. Chem. Soc.* **2000**, 122 (29), 6917. doi:10.1021/ja000617g.
- (38) Bichler, P.; Chalifoux, W. A.; Eisler, S.; Shi Shun, A. L. K.; Chernick, E. T.; Tykwinski, R. R. *Org. Lett.* **2009**, 11 (3), 519. doi:10.1021/ol8023665.
- (39) Wasylshen, R. E. *Annu. Rep. Nucl. Magn. Reson. Spectrosc.* **1977**, 7, 245.
- (40) Bohlmann, F.; Brehm, M. *Chem. Ber.* **1979**, 112 (3), 1071. doi:10.1002/cber.19791120330.
- (41) Wakabayashi, T.; Tabata, H.; Doi, T.; Nagayama, H.; Okuda, K.; Umeda, R.; Hisaki, I.; Sonoda, M.; Tobe, Y.; Minematsu, T.; Hashimoto, K.; Hayashi, S. *Chem. Phys. Lett.* **2007**, 433 (4-6), 296. doi:10.1016/j.cplett.2006.11.077.
- (42) (a) Burri, E.; Diederich, F.; Nielsen, M. B. *Helv. Chim. Acta* **2001**, 85 (7), 2169. doi:10.1002/1522-2675(200207)85:7<2169::AID-HLCA2169>3.0.CO;2-Z; (b) Zhao, Y.; Campbell, K.; Tykwinski, R. R. *J. Org. Chem.* **2002**, 67 (2), 336. doi:10.1021/jo015810n; (c) Zhao, Y. M.; Zhou, N. Z.; Slepko, A. D.; Ciulei, S. C.; McDonald, R.; Hegmann, F. A.; Tykwinski, R. R. *Helv. Chim. Acta* **2007**, 90 (5), 909. doi:10.1002/hlca.200790092; (d) Zhao, Y. M.; Slepko, A. D.; Akoto, C. O.; McDonald, R.; Hegmann, F. A.; Tykwinski, R. R. *Chem. Eur. J.* **2004**, 11 (1), 321. doi:10.1002/chem.200400822.
- (43) (a) Eisler, S.; Chahal, N.; McDonald, R.; Tykwinski, R. R. *Chem. Eur. J.* **2003**, 9 (11), 2542. doi:10.1002/chem.200204584; (b) Shi Shun, A. L. K.; Chernick, E. T.; Eisler, S.; Tykwinski, R. R. *J. Org. Chem.* **2003**, 68 (4), 1339. doi:10.1021/jo026481h.
- (44) Orendt, A. M.; Facelli, J. C.; Jiang, Y. J.; Grant, D. M. *J. Phys. Chem. A* **1998**, 102 (39), 7692. doi:10.1021/jp981079l.
- (45) Chalifoux, W. A.; McDonald, R.; Ferguson, M. J.; Tykwinski, R. R. *Angew. Chem. Int. Ed.* **2009**, 48 (42), 7915. doi:10.1002/anie.200902760.
- (46) Bennett, A. E.; Rienstra, C. M.; Auger, M.; Lakshmi, K. V.; Griffin, R. G. *J. Chem. Phys.* **1995**, 103 (16), 6951. doi:10.1063/1.470372.
- (47) Earl, W. L.; VanderHart, D. L. *J. Magn. Reson.* **1982**, 48, 35.
- (48) Gan, Z.; Roy, R. *Tetrahedron Lett.* **2000**, 41 (8), 1155. doi:10.1016/S0040-4039(99)02285-6.
- (49) Müller, T. J. J.; Robert, J. P.; Schmäzlin, E.; Bräuchle, C.; Meerholz, K. *Org. Lett.* **2000**, 2 (16), 2419. doi:10.1021/ol006048z.
- (50) Doisneau, G.; Balavoine, G.; Fillebeen-Khan, T. *J. Organomet. Chem.* **1992**, 425 (1-2), 113. doi:10.1016/0022-328X(92)80026-T.